



Universiteit
Leiden
The Netherlands

Inhibition of transcription leads to rewiring of locus-specific chromatin proteomes

Poramba-Liyanage, D.W.; Korthout, T.; Cucinotta, C.; Kruijsbergen, I. van; Welsem, T. van; Atmioui, D. el; ... ; Leeuwen, F. van

Citation

Poramba-Liyanage, D. W., Korthout, T., Cucinotta, C., Kruijsbergen, I. van, Welsem, T. van, Atmioui, D. el, ... Leeuwen, F. van. (2020). Inhibition of transcription leads to rewiring of locus-specific chromatin proteomes. *Genome Research*, 30(4), 635-646.
doi:10.1101/gr.256255.119

Version: Publisher's Version
License: [Creative Commons CC BY 4.0 license](https://creativecommons.org/licenses/by/4.0/)
Downloaded from: <https://hdl.handle.net/1887/3181186>

Note: To cite this publication please use the final published version (if applicable).

RSC primes the quiescent genome for hypertranscription upon cell cycle re-entry

Christine E. Cucinotta, Rachel H. Dell, Kean C.A. Bracerros, and Toshio

Tsukiyama*

Division of Basic Sciences, Fred Hutchinson Cancer Research Center, Seattle WA

*To whom correspondence should be addressed.

Tel: 206-667-4996

Email: ttsukiya@fredhutch.org

1 **Abstract**

2 Quiescence is a reversible G_0 state essential for differentiation, regeneration, stem cell
3 renewal, and immune cell activation. Necessary for long-term survival, quiescent
4 chromatin is compact, hypoacetylated, and transcriptionally inactive. How transcription
5 activates upon cell-cycle re-entry is undefined. Here we report robust, widespread
6 transcription within the first minutes of quiescence exit. During quiescence, the
7 chromatin-remodeling enzyme RSC was already bound to the genes induced upon
8 quiescence exit. RSC depletion caused severe quiescence exit defects: a global
9 decrease in RNA polymerase II (Pol II) loading, Pol II accumulation at transcription start
10 sites, initiation from ectopic upstream loci, and aberrant antisense transcription. These
11 phenomena were due to a combination of highly robust Pol II transcription and severe
12 chromatin defects in the promoter regions and gene bodies. Together, these results
13 uncovered multiple mechanisms by which RSC facilitates initiation and maintenance of
14 large-scale, rapid gene expression despite a globally repressive chromatin state.

15

16 **Introduction**

17 For decades scientists have used budding yeast to uncover mechanisms of chromatin
18 regulation of gene expression; and the vast majority of these studies were performed in
19 exponentially growing (hereafter log) cultures [1]. Log phase, however, is not a common
20 growth stage in unicellular organism lifecycles. Furthermore, many cell populations in
21 multicellular organisms, such as in humans, are not actively dividing [2–4]. Indeed, the
22 majority of “healthy” cells on Earth are not sustained in a persistently dividing state [3].
23 Non-proliferating cells reside in a G_0 state, which generally means these cells are either

24 terminally differentiated, senescent, or quiescent. The quiescent state provides
25 advantages to organisms: quiescence allows cells to remain dormant for long periods of
26 time to survive harsh conditions or to prevent over-proliferation [3–5,2]. Notwithstanding
27 this so-called “dormant state”, quiescent cells can exit quiescence and re-enter the
28 mitotic cell-cycle in response to growth cues or environmental stimuli, which
29 distinguishes quiescence from other G_0 states. A major hallmark of quiescence is the
30 chromatin landscape—vast histone de-acetylation and chromatin compaction occur
31 during quiescence entry [6–8]. These events happen alongside a global narrowing of
32 nucleosome depleted regions (NDR) and increased resistance to micrococcal nuclease
33 (MNase) digestion, indicating a repressive chromatin environment [6]. Together, these
34 features of quiescent cells point to a critical role for chromatin regulation of the
35 quiescent state. However, the role of chromatin regulation upon exit from quiescence is
36 unknown.

37 Reversibility is a conserved hallmark of quiescent cells and is required for proper
38 stem-cell niche maintenance, T-cell activation, and wound healing in metazoans [4,9].
39 Therefore, we sought to elucidate molecular mechanisms by which cells can overcome
40 this repressive chromatin environment to re-enter the mitotic cell cycle. Given its genetic
41 tractability, the ease by which quiescent cells can be purified, and high level of
42 conservation among chromatin and transcription machinery, we turned to the budding
43 yeast *Saccharomyces cerevisiae* [10]. We can easily isolate quiescent yeast cells after
44 seven days of growth and density-gradient centrifugation. In this context, we can study
45 pure populations of quiescent yeast, a cell fate that is distinct from other cell types
46 present in a saturated culture [11].

47 Since DNA is wrapped around an octamer of histone proteins in increments of
48 ~147bp to form nucleosomes [12], enzymes must move nucleosomes to give access to
49 transcription initiation factors [13]. One such enzyme is the SWI/SNF-family member,
50 RSC, which is a 17-subunit chromatin remodeling enzyme complex [14]. RSC contains
51 an ATP-dependent translocase, Sth1 [15–18], multiple subunits with bromodomains
52 (more than half of all bromodomains in the yeast genome are in RSC) and two zinc-
53 finger DNA-binding domains, which allow RSC to target and remodel chromatin [19,20].
54 Many components of the RSC complex are essential for viability in budding yeast and
55 the complex is conserved in humans, where it is named PBAF. In humans, mutations in
56 PBAF genes are associated with 40% of kidney cancers [21]; and 20% of all human
57 cancers contain mutations within SWI/SNF family genes [22], underscoring the
58 importance of such complexes in human health.

59 The best-described role for RSC in regulating chromatin architecture and
60 transcriptions is its ability to generate NDRs, by sliding or evicting nucleosomes [23–25].
61 Moving the +1 nucleosome allows for TATA binding protein (TBP) promoter binding and
62 transcription initiation [26]. To this end, RSC mostly localizes to the -1, +1, and +2
63 nucleosomes in log cells [27–29]. However, RSC has also been implicated in the
64 transcription elongation step where it tethers to RNA polymerase and can localize to
65 gene bodies [30–32]. Additionally, RSC binds nucleosomes within the so-called “wide
66 NDRs”, where there are MNase-sensitive nucleosome-sized fragments, known as
67 “fragile” nucleosomes [33–36]. These RSC-bound nucleosomes are likely partially
68 unwrapped to aid in rapid gene induction [36–39].

69 In this study, we investigated how genes are transcribed during the first minutes
70 of quiescence exit. We were particularly interested in uncovering mechanisms to
71 overcome highly repressive chromatin found in quiescent cells. Unexpectedly, ~60% of
72 the yeast genome was transcribed by RNA polymerase II (Pol II) by the first 10-minutes
73 of exit, despite the highly repressive chromatin architecture present in quiescence. We
74 found that this hypertranscription [40] event is RSC dependent and that RSC binds
75 across the genome to ~80% of NDRs in quiescent cells. Upon RSC depletion, we
76 observed canonical abrogation of transcription initiation, defects in Pol II clearance past
77 the +1 nucleosome, and gross Pol II mislocalization, resulting in abnormal upstream
78 initiation and aberrant non-coding antisense transcripts. We further showed that RSC
79 alters chromatin structure to facilitate these processes. Taken together, we propose a
80 model in which RSC is bound to NDRs in quiescent cells to facilitate robust and
81 accurate burst of transcription upon quiescent exit through multiple mechanisms.

82

83 **Results**

84 **Hypertranscription occurs within minutes of nutrient repletion post-quiescence**

85 To determine the earliest time at which transcription reactivates during
86 quiescence exit, we fed purified quiescent cells YPD medium and took time points to
87 determine the kinetics of Pol II C-terminal domain (CTD) phosphorylation by western
88 blot analysis (Fig. 1A). Unexpectedly, Pol II CTD phosphorylation occurred within three
89 minutes (Fig. 1A, compare lanes 1 and 2), which was our physical limit of isolating cells
90 during this time course. To determine which transcripts were generated during these
91 early quiescence exit events, we performed nascent RNA-seq using 4-thio-uracil (4tU)

92 to metabolically label new transcripts [41,42]. In agreement with the western-blot
93 analysis, we observed a high level of transcriptional activation within a few minutes of
94 nutrient repletion (Fig. 1B). Based on our western-blot result, the highest Pol II CTD
95 phosphorylation is observed ~ten minutes after refeeding. Consistent with this result, we
96 observed the highest level of nascent transcripts at the ten-minute time point, where
97 ~1000 mRNAs (20% of the genome) were statistically significantly increased compared
98 to the zero-minute time point (Fig.1B, Fig.1—supplement 1A). Given how quickly Pol II
99 was phosphorylated and transcripts were generated, we sought to determine if high
100 levels of Pol II were already bound to the early exit genes in the quiescent state, as was
101 observed previously in a heterogenous population of stationary phase cells [43]. To this
102 end, we performed spike-in-normalized ChIP-seq analysis of Pol II in quiescent cells
103 and at several time points following refeeding (Fig. 1C, Fig. 1—supplement 1B). Low
104 Pol II occupancy levels (compare heatmaps 1 and 5) were detected in quiescent cells,
105 which agrees with our western blot and RNA-seq analyses and previously published
106 literature [6–8]. This implied that Pol II is not paused (Fig. 1C, compare heatmaps 1 and
107 2) in quiescent cells, and suggested that Pol II needs to be recruited *de novo* for rapid
108 initiation and elongation. In support of this conclusion, we detected only low levels of the
109 pre-initiation complex subunit TFIIB bound to genes in quiescent cells, which increased
110 ~3-fold by five minutes of exit (Fig. 1—supplement 1C).

111 Highlighting the high level of transcription occurring in the first ten minutes of
112 quiescence exit, we observed a drop-off in Pol II occupancy levels around the first G2/M
113 phase (240 minutes) (Fig. 1C-D, Fig. 1—supplement 1D). Indeed, when the data were
114 sorted into k-means clusters across the time course, we noticed that many of the genes

115 expressed in the 240-minute time point were similar, but still not identical, to those
116 expressed in log cells, suggesting a recovery to log-like gene expression profile takes
117 hours post refeeding (Fig. 1C, compare columns 4 and 5, Fig. 1D). There was a ~1.7-
118 fold increase in overall Pol II occupancy in the 10-minute time point relative to that of log
119 cells (Fig. 1D, Fig.1—supplement 1B). Together, these results demonstrate transcription
120 activates extremely rapidly and robustly in response to nutrient repletion.

121

122 **Chromatin bears hallmarks of repression during early quiescent exit time points**

123 Given the exceptionally high transcriptional response during the first ten minutes of
124 quiescence exit, we wondered whether chromatin changes reflected hypertranscription.
125 To this end, we performed ChIP-seq analysis of H3 to measure nucleosome occupancy
126 levels genome wide over time. Global H3 patterns during the early exit time points,
127 especially at the 5-minute time point, were more similar to that of the quiescent state
128 than to the 240-minute time point (Fig. 2A, compare columns 1-3), despite higher
129 transcription levels. The most striking changes in histone occupancy during the early
130 time-points were within NDRs, where the pattern at the 10-minute timepoint resembles
131 the 240-minute time point (Fig. 2A, B). However, the H3 profiles outside of NDRs (Fig.
132 2A, compare column 1-3 and 4 to the right of NDR, and Fig.2B) remain similar to that of
133 quiescent state during the early stage of quiescent exit. In addition to nucleosome
134 occupancy, we tested nucleosome positioning using MNase-seq analysis where
135 nucleosomes with 80% of the digested chromatin is represented by mononucleosomes.
136 Globally, nucleosome positions were stable across the early exit time points (Fig. 2C).

137 We next tested if a burst of histone acetylation occurred during these early exit
138 time points to help overcome the repressive quiescent chromatin environment. To test
139 this, we performed ChIP-seq analysis of H4ac using an antibody that recognizes penta-
140 acetylated H4. Similar to nucleosome occupancy and positions, a modest increase in
141 histone H4 acetylation occurred, but the levels did not reflect that of log cells (Fig. 2D,
142 E). This suggests that, while there was a strong transcriptional response during
143 refeeding, histone acetylation was delayed. This is consistent with a previous study of a
144 mixed population of saturated cultures where histone acetylation was found to occur
145 later in exit[44]. Together, our results are in agreement with a recent study
146 demonstrating that histone acetylation takes place mostly as a consequence of
147 transcription [45].

148 To assess a biological readout of the repressive chromatin environment, we
149 turned to phenotypic analysis of TFIIS disruption. TFIIS is a general elongation factor
150 that rescues stalled Pol II; and nucleosomal barriers have been shown to increase
151 stalled Pol II [46]. Given that Pol II stalling is common across the genome [47], it is
152 paradoxical that the gene encoding TFIIS is not essential for viability in actively dividing
153 cells, and its deletion does not cause strong growth defects [48]. Since Pol II must
154 achieve a high level of transcription in the repressive chromatin environment during
155 early quiescence exit, we hypothesized that TFIIS may play more critical roles during
156 this period than during log culture. Indeed, in the absence of TFIIS (*dst1Δ*), quiescent
157 yeast cells exhibited defects in cell cycle re-entry, where cells lacking TFIIS stall at the
158 first G1 during exit, which is not the case during the mitotic cell cycle (Fig. 2F, Fig. 2—

159 supplement 1B). These results collectively revealed that the chromatin environment
160 remains repressive during early quiescence exit.

161

162 **In quiescence, RSC re-localizes to NDRs of genes expressed in exit**

163 Given the modest changes in chromatin at most genes during the early stage of
164 quiescence exit (Fig. 2), we wondered whether MNase-sensitive or “fragile”
165 nucleosomes were present at the promoters of rapidly induced genes in quiescence and
166 were removed in early exit. Thus, we performed a weaker (low) MNase digestion (10%
167 mononucleosomes) (Fig. 3A) and compared it to the stronger (high) MNase digestion
168 (80% mononucleosomes) (Fig. 3B). Supporting our hypothesis, comparing the weaker
169 MNase digest to the stronger MNase digest revealed that ~1000 genes have fragile
170 nucleosomes in quiescent cells, which are reduced during exit (Fig. 3A). Additionally,
171 we noticed that the MNase-sensitivity of the +1 and +2 nucleosomes increased at the
172 10-minute time point, likely coinciding with transcription.

173 It has been recently suggested that that the ATP-dependent chromatin remodeler
174 RSC can remove fragile nucleosomes from promoters to activate transcription [26].
175 Additionally, it was proposed that RSC-bound nucleosomes are remodeling
176 intermediates that render such nucleosomes more MNase-sensitive [38]. Thus, RSC
177 was a strong candidate for regulating rapid transcription activation during quiescence
178 exit. We performed ChIP-seq analysis of the RSC catalytic subunit Sth1 in quiescent
179 cells. In quiescence, Sth1 exhibited a striking difference in binding pattern compared to
180 log cells (Fig. 3C, D). Sth1 bound to ~80% of NDRs at gene promoters in quiescent
181 cells (Fig. 3E, Figure 3—supplement 1A). This result was distinct from log cells, where

182 RSC was reported to occupy the widest NDRs but otherwise bind the -1, +1, and +2
183 nucleosomes for most highly expressed genes (Fig. 3C) [28,26,38]. The RSC binding
184 pattern in quiescent cells instead mirrored a recently described binding pattern in heat
185 shock, where RSC and other transcription regulators *transiently* relocate to the NDRs
186 [49]. In contrast to the heat shock response, however, we observed a stable, strong
187 binding pattern of RSC in NDRs regardless of NDR width (Fig. 3E). Another obvious
188 distinction of RSC binding patterns between log and quiescence was observed at tRNA
189 genes (Fig. 3F). RSC's role at tRNA expression has been well-studied in log cells [50–
190 52]. In quiescence, RSC was occluded from tRNAs genes. Whereas upon exit, RSC
191 rapidly targeted tRNAs, mimicking the log pattern. Together these data suggest that
192 RSC adopts a quiescence-specific binding profile, one in which RSC is bound to NDRs
193 more broadly across the genome.

194 We next sought to gain insight into how quiescent RSC occupancy patterns
195 might predict Pol II occupancy during exit. To this end, we compared localization of
196 RSC and Pol II in quiescence and exit. We first found that the presence of RSC at
197 NDRs in quiescent cells and strong transcription in exiting cells co-localized (Fig. 3—
198 supplement 1A). Next, we examined RSC occupancy changes during quiescence exit at
199 Pol II-transcribed genes. During quiescence exit, RSC began to move out of NDRs and
200 into gene bodies as transcription increased (Fig. 3G). These results suggested that
201 RSC facilitates transcriptional activation upon exit and raised the possibility that RSC
202 binding in NDRs may be a mechanism for cells to prepare for quiescence exit.

203

204 **RSC depletion causes quiescent exit defects and global Pol II occupancy**
205 **reduction during quiescence exit**

206 To test the requirement of RSC in quiescence exit, we simultaneously depleted two
207 essential subunits of the RSC complex, Sth1 and Sfh1, using the auxin degron system
208 [53], during quiescence entry (see methods; Figure 3—supplement 1B). Depletion of
209 these subunits throughout the exit process (hereafter “-RSC”) caused a dramatic defect
210 in cell cycle progression upon quiescence exit, where the cells exhibited strong delays
211 in exiting the first G1 stage (Figure 4A). This result contrasted with that in cycling cells,
212 where *rsc* mutants or conditional alleles cause G2/M arrest [54].

213 To determine the impact of RSC depletion on hypertranscription during
214 quiescence exit, we performed Pol II ChIP-seq analysis on cells exiting quiescence. In
215 the presence of RSC, Pol II levels peaked at 10 minutes and substantially decreased at
216 30 minutes after the exit (Fig. 4B, compare columns 3 and 4). As is the case in log
217 cultures [50,55,56], Pol II occupancy decreased in the absence of an intact RSC
218 complex in Q-cells and upon nutrient repletion thereafter (Fig. 4B). Pol II occupancy did
219 eventually increase over time in the RSC-depleted samples. However, even after 30-
220 minutes, Pol II did not reach the peak level of occupancy seen at the 10-minute mark in
221 the +RSC condition (Fig. 4B, compare heatmaps 3 and 8, and 4C). This suggests that
222 the defect in Pol II occupancy during quiescence exit was not solely due to slower
223 kinetics.

224 As shown earlier in Figure 3G, we observed RSC leaving the NDRs and moving
225 into gene bodies during quiescence exit. Therefore, we examined the impact of RSC
226 depletion on nucleosome occupancy and positioning. H3 ChIP-seq showed that RSC is

227 required for removal of histones within NDRs (Fig. 4D), which is consistent with RSC's
228 role as the “NDR creator” [24]. Together, these data provide mechanistic explanations
229 for how RSC facilitates Pol II loading during early stages of quiescence exit.

230

231 **RSC is required for Pol II passage through gene bodies**

232 Given that RSC moves from NDRs into gene bodies during quiescence exit (Fig. 3G),
233 we next tested whether RSC could aid transcription after initiation. To this end, we
234 selected ~2000 genes where RSC moved toward gene bodies and examined RSC
235 localization at the 10-minute time point of quiescent exit. This analysis showed uniform
236 movement of RSC from NDR into gene bodies (Fig. 5A). We next tested whether this
237 RSC movement is dependent on Pol II transcription. To this end, we performed Sth1
238 ChIP-seq analyses during quiescence exit in the presence of a transcription inhibitor
239 1,10-phenanthroline (Fig. 5B, Pol II control in Fig. 5—supplement 1A). This experiment
240 demonstrated that the movement of RSC from NDRs into gene bodies was strongly
241 inhibited by 1,10-phenanthroline, establishing that RSC re-localization during quiescent
242 exit is dependent on Pol II transcription.

243 Co-transcriptional movement of RSC into gene bodies suggested a possibility
244 that RSC may help Pol II passage through gene bodies. To test this, we determined the
245 effects of RSC depletion on Pol II localization during early time points of quiescent exit.
246 Fig. 5C and D show that RSC depletion affects Pol II localization in at least two ways
247 during early quiescent exit. First, consistent with Fig 4B, the robust increase in the
248 amount of Pol II over genes is strongly decreased upon RSC depletion. In addition,
249 upon RSC depletion, Pol II sharply accumulates at TSSs at the 5-minute mark, which

250 continued to the 10-minute mark. In sharp contrast, Pol II accumulates at slightly more
251 downstream at the 5-minute mark and moves mostly to downstream regions at the 10-
252 minute time point in the presence of RSC. We also noticed a pile-up of Pol II at the 3'-
253 end of genes at the 5-minute timepoint upon RSC depletion (Fig. 5C). This is in
254 agreement with the possibility that RSC may be involved in proper transcription
255 termination [57]. At these loci, NDRs are relatively shallow in quiescence but histone
256 density rapidly decreases upon quiescence exit in the presence of RSC (Fig. 5E, Fig.
257 5—supplement 1B). In the absence of RSC at these sites, however, histone density is
258 unexpectedly lower at NDR in quiescence but does not change during quiescent exit
259 (Fig. 5F, Fig. 5—supplement 1B), suggesting defective chromatin structure at and
260 downstream of the NDR. Together, these results are consistent with the notion that co-
261 transcriptional movement of RSC facilitates passage of Pol II through nucleosomes
262 immediately downstream of TSSs through chromatin regulation.

263

264 **RSC suppresses abnormal upstream transcription initiation**

265 The fact that Pol II accumulated upstream of TSSs at the 5-minute mark upon RSC
266 depletion (Fig. 5C) suggested possible defects in transcription start site selection. To
267 test this possibility, we examined the 4tU-seq profiles of a subset of RSC targets (1426
268 genes) in which there appeared to be an enrichment of RNA signal directly upstream
269 and downstream of TSSs. We took the \log_2 ratio of RNA signal in the depleted condition
270 versus the non-depleted condition at the ten-minute time point (Fig. 6A). We sorted the
271 genes using k-means clusters and took into account RSC binding when determining
272 gene sets to analyze.

273 This analysis revealed that upon RSC depletion a large number of genes (~1400)
274 exhibited increased nascent sense-strand RNA signals starting upstream of their normal
275 TSSs, demonstrating wide-spread defects in TSS selection. Examination of individual
276 loci revealed that, in addition to filling of an NDR at the normal TSSs, an NDR is created
277 upstream, which overlaps with ectopic transcription observed at an upstream TSS (see
278 Fig. 6B for an example). These results suggest that RSC facilitates selection of accurate
279 transcription initiation sites through proper NDR formation upstream of protein coding
280 genes during the burst of transcription during quiescence exit. This is likely a
281 quiescence-specific function of RSC, or a result of the robust hypertranscription event
282 during exit, as depletion of Sth1 in cycling cells mostly repressed transcription initiation
283 with relatively few new upstream transcription start sites [55,56].

284

285 **RSC is required for suppression of anti-sense transcripts during quiescence exit**

286 Given the robust transcriptional response during the early minutes of quiescence exit
287 (Fig. 1), we examined whether aberrant transcripts might also arise during quiescence
288 exit when RSC was depleted. Indeed, in many cases we found antisense transcripts
289 arising in the absence of RSC. We found ~900 RSC targets that had generally reduced
290 sense transcript levels with strongly upregulated cognate antisense transcripts (Class I),
291 and ~600 genes (Class II) with only modest changes in both sense and anti-sense
292 transcript levels upon RSC depletion (Fig. 7A). Chromatin analyses of individual Class I
293 loci revealed that RSC depletion caused narrower NDRs upstream of the sense TSS
294 (see Fig. 7B for an example). In contrast, NDRs for sense transcripts remained largely
295 open at Class II genes (Fig. 7B). Both classes have RSC bound at the promoters of the

296 sense genes in quiescence, with slightly higher RSC binding in the class I genes (Fig.
297 7C). Strikingly, nucleosome positioning was heavily impacted in the Class I set of genes
298 upon RSC depletion in the sense direction, where NDRs became more resistant to
299 MNase and nucleosomes in gene bodies were shifted toward the 5'-ends of genes. This
300 was in contrast to that of Class II where NDRs were largely open (Fig. 7D). Consistent
301 with the MNase-mapping data, nucleosome occupancy at NDRs and in gene bodies are
302 much more strongly affected by RSC depletion at Class I genes than Class II genes
303 (Fig. 7E). It is likely that Class II genes overcome the absence of RSC by having more
304 "fragile" nucleosomes that can be readily removed by general regulatory factors [26].
305 These results collectively showed that chromatin structure at the Class I genes is
306 especially dependent on RSC. In both classes of genes, RSC signals and RSC-
307 dependent chromatin changes are not apparent around the start sites of anti-sense
308 transcripts. Therefore, suppression of anti-sense transcripts is unlikely to be a direct role
309 for RSC. Instead, it is likely that both Class I and II genes, especially the former, have
310 an intrinsic property to allow anti-sense transcription to occur when not properly
311 regulated, and RSC is targeted to them to ensure sense transcription takes place
312 through formation of proper NDRs.

313

314 **Discussion**

315 In this report we have shown that there is a rapid and robust transcriptional response
316 during the very early minutes of quiescence exit (Fig. 8A). This response is greatly
317 dependent on the chromatin remodeling enzyme RSC. We found that RSC promotes
318 transcription at the right place and time in four different ways: 1) RSC promotes

319 transcription initiation by creating NDRs in quiescence and maintaining them during exit
320 (Fig. 8B). 2) RSC moves into gene bodies and helps Pol II transcribe past the +1
321 nucleosome (Fig. 8C). 3) RSC maintains proper NDR locations to allow for accurate
322 transcription start site selection (Fig. 8D). 4) RSC suppresses cryptic antisense
323 transcription via generating NDRs at the cognate sense genes (Fig. 8E). Together, our
324 results suggest that the massive transcriptional response requires highly accurate
325 nucleosome positioning to allow for cells to exit from the quiescent state.

326 Quiescent yeast must downregulate their transcriptional program and generate a
327 repressive chromatin environment in order to survive harsh conditions for extended time
328 periods [10,6,58,59]. How, then, do cells rapidly escape the quiescent state when
329 conditions are favorable? In this study, we show that there is an incredibly strong
330 transcriptional response to nutrient repletion after quiescence, notwithstanding a
331 relatively repressive chromatin environment that persists until the first G2/M phase after
332 quiescence. Indeed, we identified a previously unidentified phenotype for the deletion of
333 the gene encoding yeast TFIIIS, *dst1* Δ . High numbers of stalled Pol II are present in
334 cycling cells [47] despite the little impact of deleting *DST1* on cycling cell growth. We
335 speculate cells exiting quiescence may rely more heavily on TFIIIS to transcribe through
336 repressive chromatin [60,61].

337 During quiescence, RSC relocates to NDRs upstream of Pol II transcribed genes
338 that are transcribed in exit. Although RSC binds and regulates chromatin around Pol III
339 genes [27,50], RSC is depleted at tRNA genes in quiescence and only returns during
340 quiescence exit, further supporting the notion that RSC is globally re-targeted in
341 quiescence. This is distinct from the transient NDR-relocalization observed in heat

342 shock [49], as what we observed in quiescence was a sustained and rather stable
343 localization. How RSC binds to these new locations in quiescence is unknown. Given
344 the distinct structure of quiescent chromatin there are several, non-mutually exclusive,
345 explanations for RSC's binding pattern in quiescence. 1) The genome is hypoacetylated
346 and thus RSC can no longer bind to acetylated nucleosomes in quiescence via its
347 bromodomains [19]. However, given the highly robust response to refeeding, RSC
348 activity must be poised to be active in this state. An intriguing possibility could be that
349 histone acetylation inhibits RSC activity to some extent as was recently reported *in vitro*
350 [62]. This would be consistent with the rapid changes in nucleosome positioning at
351 many genes during quiescence exit in the absence of high levels of histone acetylation.
352 2) Recent structural studies have shown that the nucleosome acidic patch is in direct
353 contact with subunits of the RSC complex [63–66]. If the acidic patch is occluded by
354 hypoacetylated H4 tails in quiescence for example [12,67–70], it is possible that RSC
355 can no longer interact with this region of the nucleosome, rendering its binding abilities
356 different in quiescence. Finally, 3) a lack of Pol II activity in quiescent cells could prevent
357 RSC from moving out of NDRs and into gene bodies. Indeed, transcription appears to
358 play a prominent role in RSC localization: RSC moves into gene bodies during
359 transcription activation and this movement is blocked when transcription is inhibited, as
360 we have reported above. It is likely that a combination of transcription and histone
361 acetylation helps pull RSC into gene bodies, given recent work showing that acetylation
362 is a consequence of transcription [45]. In a separate study, we recently found that the
363 SWI/SNF remodeling enzyme promotes transcription of a subset of hypoacetylated
364 genes during quiescence entry, implying a specialized transcription regulation program

365 for essential genes in the wake of widespread transcriptional shutdown [58]. In cycling
366 cells, it was recently shown that RSC and SWI/SNF cooperate at a subset of genes
367 [71]. Our results suggested that cooperation between the two SWI/SNF class
368 remodeling factors may also occur during quiescence entry.

369 Consistent with co-transcriptional re-localization, our data suggest RSC plays an
370 active role in helping Pol II transcribe past the +1 nucleosome in addition to initiating
371 transcription. Supporting this idea was our observation of a subset of genes where RSC
372 depletion caused a Pol II enrichment around the +1 nucleosome. Previous reports
373 showed that RSC can bind gene bodies and impact elongating and terminating Pol II
374 [31,57]; and one study showed interactions between the Rsc4 subunit and all three RNA
375 polymerases [30]. An intriguing possibility could be that RSC directly interacts with Pol II
376 to facilitate transcription past the first few nucleosomes.

377 The transcriptional response during quiescent exit was dampened by depleting
378 the essential chromatin remodeler, RSC, but it did not diminish completely. Pol II
379 occupancy was globally decreased ~2-fold at the 10-minute time point in RSC-depleted
380 cells. However, at ~900 genes we found that while sense transcription was reduced,
381 antisense transcripts were generated. This was largely due to a nearby NDR
382 susceptible to transcription initiation that could be co-opted for antisense transcription.
383 The mechanism that allows for this cryptic transcription is still unknown. Chromatin
384 remodeling enzymes are vastly important for repressing antisense lncRNAs [72].
385 Different chromatin remodeling enzymes function to repress lncRNA transcripts in
386 cycling cells, including RSC [73–75]. We speculate RSC is particularly suitable to
387 regulate global transcriptome during quiescence exit due to its high abundance, which

388 allows it to function through multiple mechanisms. The mouse embryonic stem cell-
389 specific BAF complex was also recently shown to globally repress lncRNA expression
390 [76]. This raises the possibility that some of our observations in yeast quiescent cells
391 could be conserved in mammalian quiescent cells. Given the robust transcriptional
392 response that occurs during quiescence exit, it is likely that chromatin structure is
393 crucial for maintaining the quality of the transcriptome. Indeed, we noted cases where
394 transcription occurred upstream of the canonical TSS when an NDR was not generated,
395 highlighting the defects in Pol II initiation and start site selection due to chromatin
396 defects in the absence of RSC. Hypertranscription events similar to the one observed
397 during quiescence exit occur throughout all organisms, particularly during development
398 [40]. Therefore, it is quite possible that we will see similar, multifaceted roles for RSC
399 homologues or other abundant chromatin remodeling factors in facilitating proper
400 hypertranscription in many other systems.

401

402 **Materials and Methods**

403 **Yeast strains, yeast growth media, quiescent cell purification, and exit time** 404 **courses**

405 The *S. cerevisiae* strains used in this study are listed in Supplementary Table S1 and
406 are isogenic to the strain W303-1a with a correction for the mutant *rad5* allele in the
407 original W303-1a [77]. Yeast transformations were performed as previously described
408 [78]. All cells were grown in YPD medium (2% Bacto Peptone, 1% yeast extract, 2%
409 glucose). We note that quiescent (Q) yeast need to be grown in YPD using “fresh”
410 (within ~three months) yeast extract as a source. To purify Q cells, liquid YPD cultures

411 were inoculated with a single colony into liquid cultures (colonies were no older than
412 one week). Yeast cells were grown in Erlenmeyer flasks ten times the liquid volume for
413 seven days at 30°C and shaking at 180 RPM. Q cells were purified by percoll gradient
414 centrifugation as previously described [11]. Briefly, percoll was diluted 9:1 with 1.5 M
415 NaCl into 25-mL Kimble tubes and centrifuged at 10,000 RPM for 15-minutes at 4°C.
416 Seven-day cultures were pelleted, washed with ddH₂O, resuspended in 1 mL of
417 ddH₂O, and gently pipetted over a pre-mixed percoll gradient. 400 OD₆₆₀ were pipetted
418 onto a 25-mL gradient. Gradients with loaded cells were centrifuged for one hour at
419 1000 RPM, 4°C. The upper, non-quiescent cell population and the middle, ~8 mL
420 fraction, were carefully discarded via pipetting. The remaining volume was washed
421 twice with ddH₂O in a 50 mL conical tube at 3,000 RPM, 10 minutes each.

422 Q exit experiments were performed as follows: Q cells were harvested and
423 added to YPD to 1 OD₆₆₀/mL. Cells were grown at 25°C to slow the kinetics for
424 feasibility. For ChIP-seq and MNase-seq experiments, cells were grown to the
425 appropriate time and then crosslinked for 20 minutes (described in more detail in the
426 sections below).

427

428 **Depletion of RSC subunits, Sth1 and Sfh1**

429 The yeast strains YTT 7222 and 7224 were grown in 5-mL overnight YPD cultures, back
430 diluted for four doublings, and inoculated to 0.002 OD₆₆₀ into the appropriate YPD
431 volume for a given experiment. Cells were grown for 16 hours and monitored for
432 glucose exhaustion using glucose strips. Six hours after glucose exhaustion, 1mg/mL of
433 Indole-3-acetic acid (Sigma, I3750-5G-A) was added, in powder form, to the culture. Q

434 cells were purified as described above and depletion efficiency was determined by
435 western blot analysis (Supplementary Figure 1A).

436

437 **Western Blot Analysis**

438 Yeast cells were lysed by bead beating in trichloroacetic acid (TCA), as previously
439 described [79]. Proteins were resolved on 8% polyacrylamide gels and transferred to
440 nitrocellulose membranes. Membranes were incubated with primary antibodies: anti-
441 Rpb3 (Biolegend, 665003 1:1000 dilution), anti-Ser5p (Active Motif, 61085 1:1000
442 dilution), anti-Ser2p (Active Motif, 61083, 1:1000 dilution), and anti-HSV (Sigma, 1:500).
443 Following primary incubation, membranes were incubated with either anti-mouse or
444 anti-rabbit secondary antibodies (Licor, 1:10000). Protein signals were visualized by the
445 Odyssey CLx scanner.

446

447 **ChIP-seq**

448 100 OD₆₆₀ U of cells were crosslinked and sonicated in biological duplicate using the
449 protocol described in [80]. Proteins were immunoprecipitated from 1 µg chromatin and 1
450 µL of anti-H3 (Abcam, 1791) conjugated to 20 µl protein G magnetic beads (Invitrogen,
451 10004D) per reaction. For Pol II ChIPs, we used an antibody against the Rpb3 subunit
452 (2 µl per reaction, Biolegend 665004) conjugated to 20 µl protein G magnetic beads
453 (Invitrogen, 10004D). For Sth1 ChIP experiments we used an antibody against the Flag-
454 epitope tag, FLAG M2 mouse monoclonal (Sigma Aldrich, F1804) and conjugated to 20
455 µl protein G beads (Invitrogen, 10004D) Libraries were generated using the Ovation
456 Ultralow v2 kit (NuGEN/Tecan, 0344) and subjected to 50-bp single-end sequencing on

457 an Illumina HiSeq 2500 at the Fred Hutchinson Cancer Research Center genomics
458 facility. We used bowtie2 to align raw reads to the sacCer3 reference genome [81].
459 Reads were then filtered using SAMtools [82]. Bigwig files of input-normalized ChIP-seq
460 data were generated from the filtered bam files using deepTools2 [83] and dividing the
461 IP data by the input data. Matrices for metaplots were generated in deepTools2 using
462 the annotation file from [84].

463

464 **MNase-seq**

465 Cell growth and crosslinking was done in the same fashion as in ChIP-seq experiments.
466 Generally, we followed the protocol in [80], with changes described here. Cells were
467 spheroplasted using 10 mg zymolyase (100T, AMSBIO, 120493-1) per 100 OD₆₆₀ cells.
468 For Q cells, zymolyase treatment could take up to two hours. We monitored the cells via
469 microscopy and stopped the spheroplasting step when ~80% of the cells were
470 spheroplasted. MNase digestion was performed as described in [80]. High digests (80%
471 mononucleosomes) required 50U of micrococcal nuclease (Worthington, LS004798)
472 and for the low digests, chromatin was treated with 10 U of MNase. From this step,
473 chromatin was reverse crosslinked as described in [80]. Following reverse crosslinking,
474 RNase, and proteinase-K digestion, DNA was phenochloroform-extracted. Any large,
475 uncut genomic DNA species was separated out using Ampure beads (Beckman).
476 Sequencing libraries were generated from the purified DNA using the Ovation Ultralow
477 v2 kit (NuGEN, 0344). Libraries were subjected to 50-bp paired-end sequencing on an
478 Illumina HiSeq 2500 at the Fred Hutchinson Cancer Research Center genomics facility.
479 We used bowtie2 to align raw reads to the sacCer3 genome and filtered reads using

480 SAMtools as described above for ChIP-seq analysis. Bigwig files of input-normalized
481 ChIP-seq data were similarly generated from the filtered bam files using deepTools2
482 and the MNase option to center the reads around nucleosome dyads. Data represented
483 in the paper were filtered to mononucleosome sizes using deepTools2.

484

485 **Nascent RNA-seq**

486 Generally, nascent RNA-seq experiments were performed as described in
487 [85,42]. For the 0-minute and 5-minute samples, we added 100 and 50 OD₆₆₀ of Q cells,
488 respectively, to YPD containing 5 mM 4-thiouracil (Sigma, 440736-1G). Cells were
489 incubated with 4tU for 5 minutes before pelleting (one minute, 3500 RPM) and flash
490 frozen in liquid nitrogen. For the 10-minute time points, 50 OD units of quiescent cells
491 were released into YPD for 5 minutes before an additional 5-minute incubation with 4tU
492 at a final concentration of 5 mM. All time points were labeled with 4tU for a total of 5
493 minutes before pelleting and freezing. Total RNA was isolated using Ambion's RiboPure
494 Yeast Kit (Thermo, AM1926). *S. cerevisiae* cells were lysed in the presence of
495 *Kluyomyces lactis* (*K. lactis*) cells in a 100:1 mixture. RNA was treated with DNaseI
496 according to the TURBO DNase kit (Thermo, AM2238). 40 ug RNA was then
497 biotinylated with MTSEA biotin-XX (diluted in 20% DMF) at a final concentration of 16.4
498 uM in 20mM HEPES pH 7.4 and 1 mM EDTA at room temperature for 30 minutes.
499 Unreacted MTS-biotin was removed from samples by PCI extraction and resuspended
500 in 100 uL nuclease-free water. Streptavidin beads (Invitrogen 65001) were washed with
501 high-salt wash buffer (100 mM Tris, 10 mM EDTA, 1 M NaCl, 0.05% Tween-20) and
502 blocked for one hour in high-salt wash buffer containing 40 ng/uL glycogen. 40 uL of

503 streptavidin beads were added to the RNA samples and incubated for 15 minutes at
504 room temperature. Beads were washed three times in 1 mL high salt wash buffer and
505 eluted for 15 minutes at room temperature in 50 uL streptavidin elution buffer (100 mM
506 DTT, 20 mM HEPES, 2.7, 1 mM EDTA, 100 mM NaCl, 0.05% Tween-20). The resulting
507 RNA was then purified and concentrated using the Qiagen miRNeasy kit (#217084).
508 Libraries were prepared from 5 ng of RNA using the Ovation SoLo kit (NuGEN/Tecan,
509 custom AnyDeplete; contact Tecan for ordering this kit for yeast). Libraries were
510 subjected to 50-bp paired-end sequencing on an Illumina HiSeq 2500 at the Fred
511 Hutchinson Cancer Research Center genomics facility. We used bowtie2 to align raw
512 reads to the *sacCer3* and *K. lactis* (Ensembl ASM251v1) genomes and filtered reads
513 using SAMtools as described above for ChIP-seq analysis. Differential expression
514 analysis was performed using DESeq2 [86]

515

516 **Data Availability**

517 All sequencing data are uploading on the NCBI Gene Expression Omnibus under the
518 accession number GSE166789.

519

520 **Acknowledgements**

521 We are grateful to members of the Tsukiyama lab and Pravrutha Raman for helpful
522 comments and critical reading of this manuscript. We thank Sarah Hainer and Felix
523 Mueller-Planitz for advice on MNase-seq experiments. We thank Benjamin Martin, Rafal
524 Donczew and Sandipan Brahma for advice and feedback. We thank Mitchell Ellison and
525 Alex Francette for advice about analyzing nascent RNA-seq data. TT was supported by

526 the National Institutes of Health (R01 GM111428 and R35GM139429). CEC was
527 supported by the National Cancer Institute (T32CA009657) and National Institutes of
528 Health (F32GM131554).

FIGURE 1

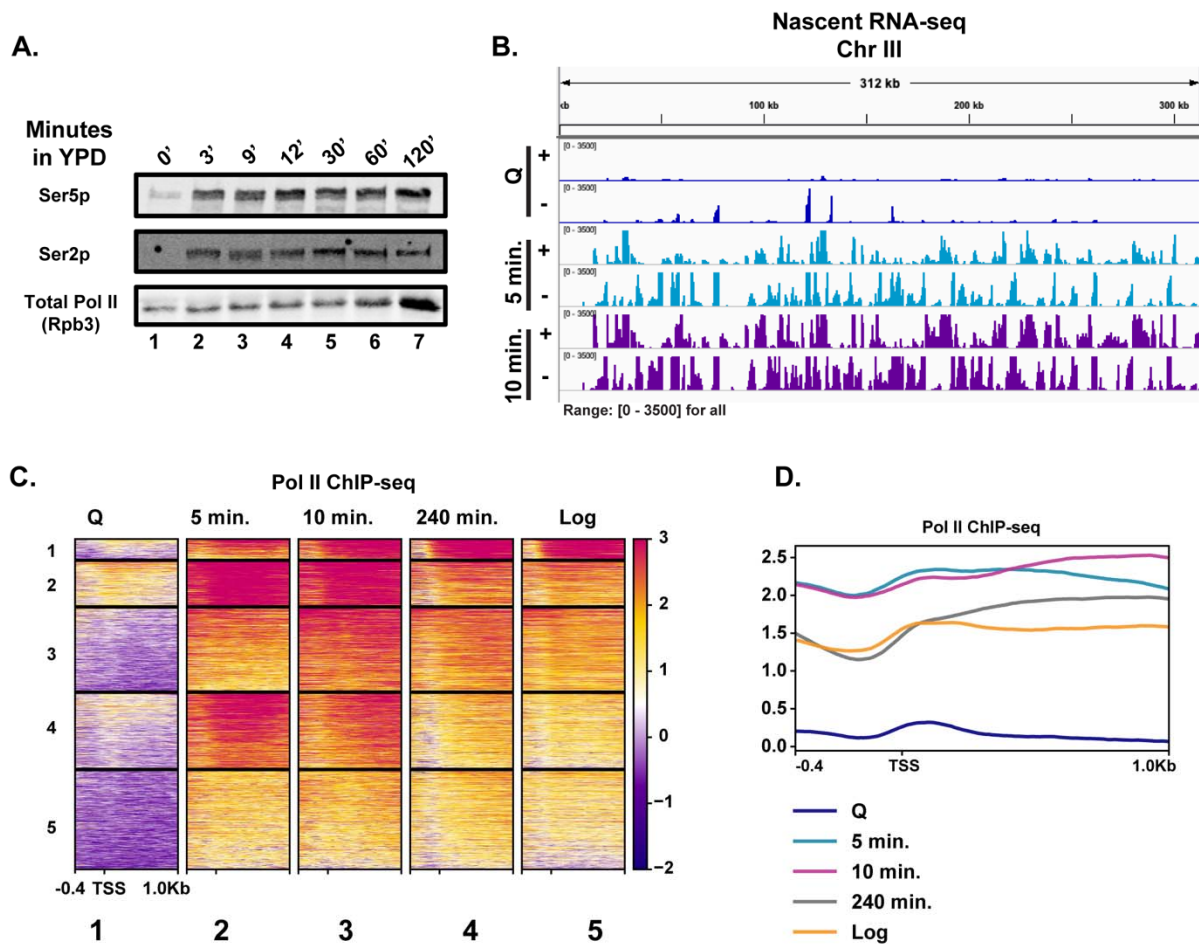


Figure 1. Rapid hypertranscription occurs upon nutrient repletion of quiescent cells

(A) Western blots were probed with antibodies to detect Ser5p and Ser2p of the CTD of Rpb1 subunit of Pol II. An antibody against the Rpb3 subunit of Pol II was used as a loading control. **(B)** Strand-specific 4tU-seq analysis. “+” indicates Watson strand and “-“ indicates Click strand. **(C)** Pol II ChIP-seq analysis. Heatmaps show k-means clusters of 6030 genes. Genes are linked across the heatmaps. **(D)** Metaplots of ChIP-seq data shown in (C) without k-means clustering.

FIGURE 1—supplement 1

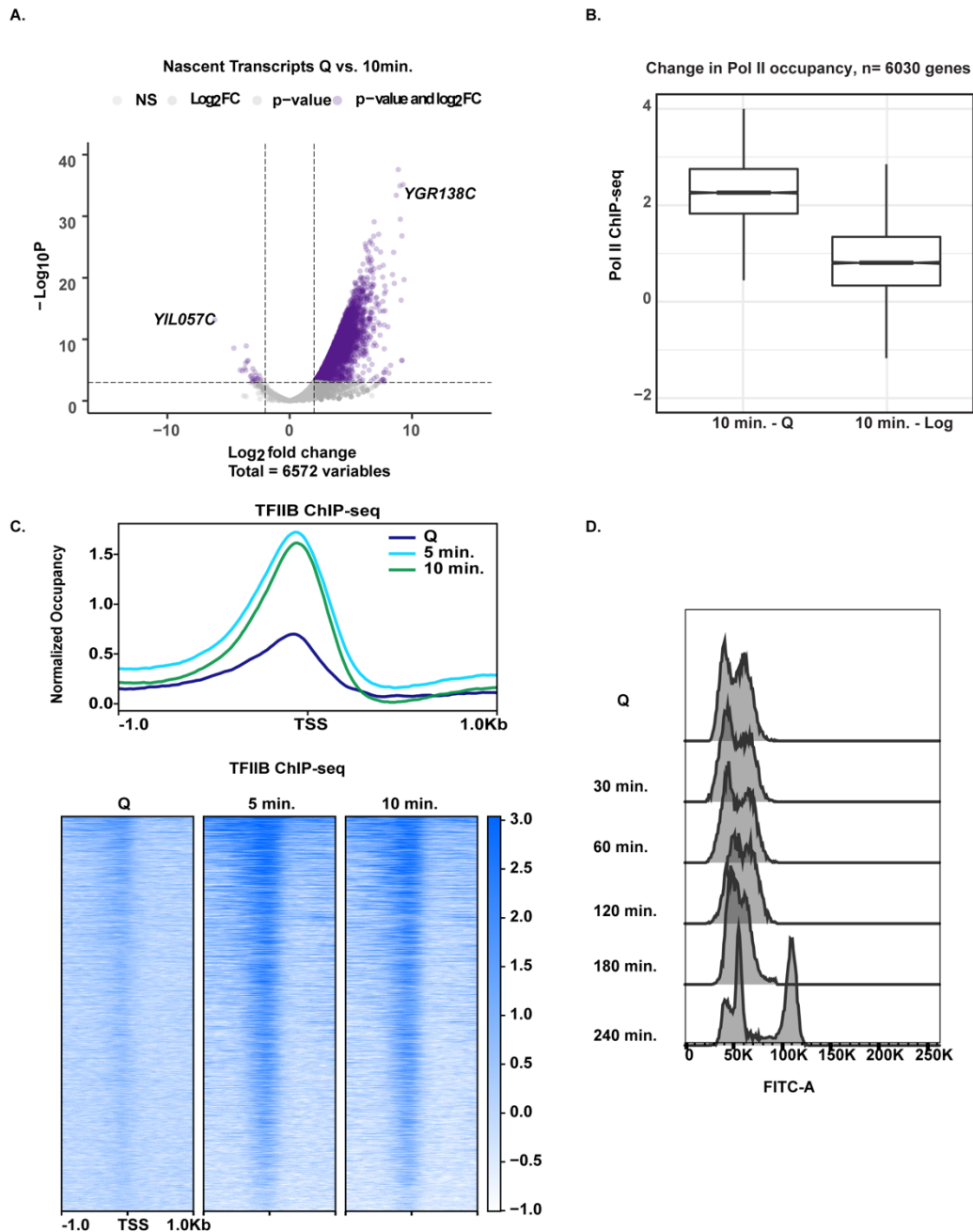


Figure 1—supplement 1

(A) Volcano plot of nascent transcripts comparing significant changes in expression using a 2-fold cut off. **(B)** Boxplots illustrating the difference in Pol II ChIP-seq signals across genes. Log_2 ratio values were subtracted (ex: Q log_2 values were subtracted from 10 min. log_2 values). **(C)** TFIIB ChIP-seq analysis in Q cells and exit time points. Genes are linked across the time points and are aligned to TSS. **(D)** DNA content FACS analysis indicating cell cycle progress during Q exit.

FIGURE 2

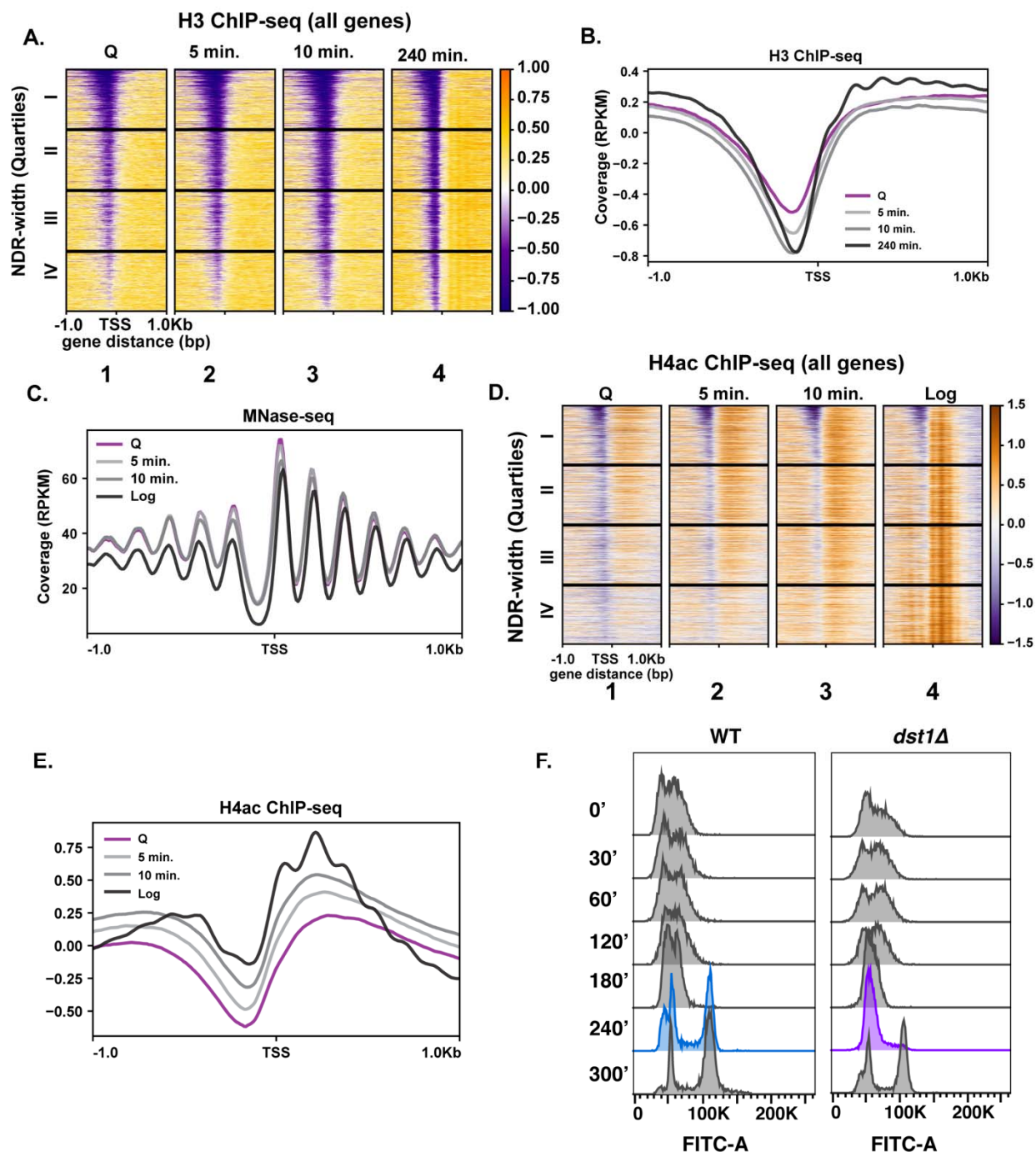


Figure 2. Repressive chromatin persists during early quiescence exit

(A, B) ChIP-seq of total H3 in quiescent cells and exit time points sorted into quartiles based on NDR width. **(C)** MNase-seq analysis of 6030 genes in Q (pink line), Log (black line), and Q-exit time points 5 minutes (light grey line) and 10 minutes (dark grey line). **(D, E)** ChIP-seq analysis of penta-acetylated H4 (H4ac) in Q and Log cells and exit time points. Genes are separated as in (B). **(F)** DNA content FACS analysis following Q exit in WT and a TFIIIS-absent strain (*dst1Δ*).

FIGURE 3

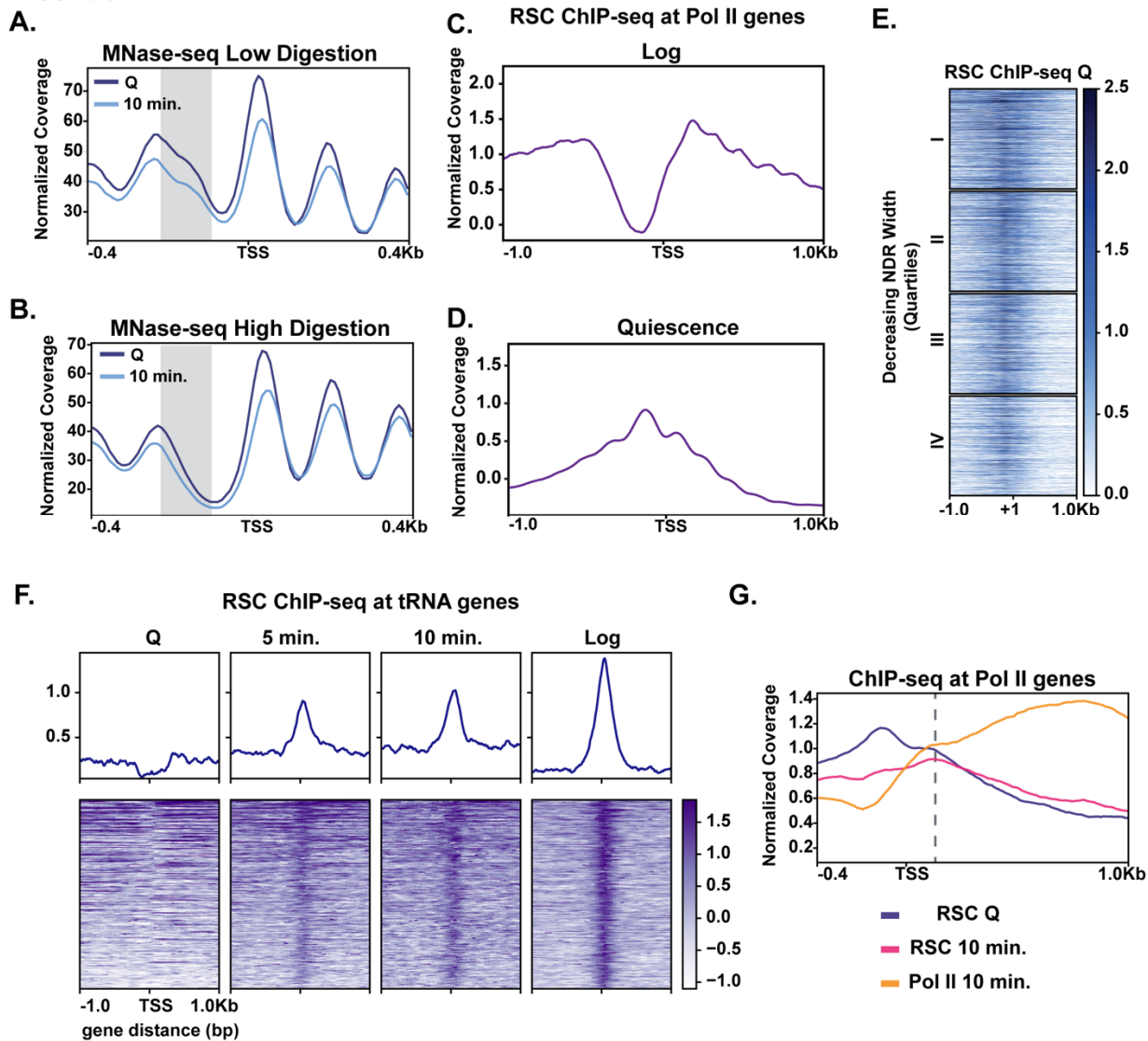


Figure 3. MNase sensitivity and quiescence-specific RSC relocalization indicate remodeling activity required for early exit

(A) MNase-digested chromatin to 10% mononucleosomes (low digestion). **(B)** Metaplot of MNase-digested chromatin to 80% mononucleosomes (high digestion) in Q and 10-minute time points. **(C,D)** ChIP-seq of the catalytic RSC subunit in quiescent and log cells at Pol II-transcribed genes. **(E)** ChIP-seq analysis of RSC shown across quartiles based on MNase-seq determined NDR width. **(F)** ChIP-seq of RSC at tRNA genes. **(G)** ChIP-seq of RSC and Pol II comparing RSC movement with Pol II into gene bodies.

FIGURE 3—supplement 1

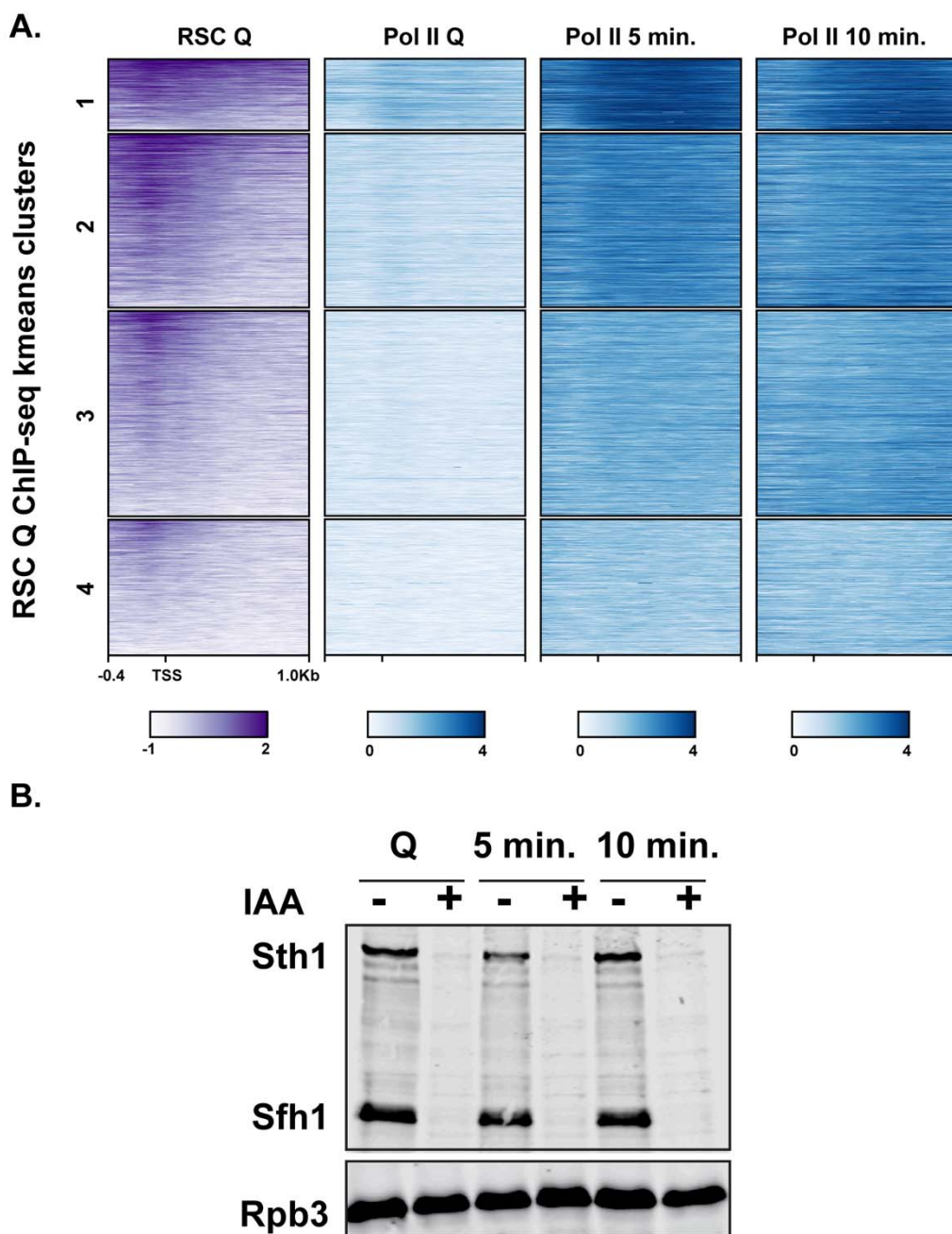


Figure 3—supplement 1

(A) ChIP-seq analysis of RSC and Pol II using antibodies against Flag-tagged Sth1 and Rpb3, respectively. Genes are sorted into k-means clustered and are linked across the different ChIPs. **(B)** Western blot analysis of RSC depletion. Both Sth1 and Sfh1 contain C-terminal HSV and AID tags for detection and depletion using IAA. Western blot was probed with an antibody recognizing the HSV epitope tag and Rpb3 (Pol II subunit) as a loading control. The addition of IAA is indicated by – or +.

FIGURE 4

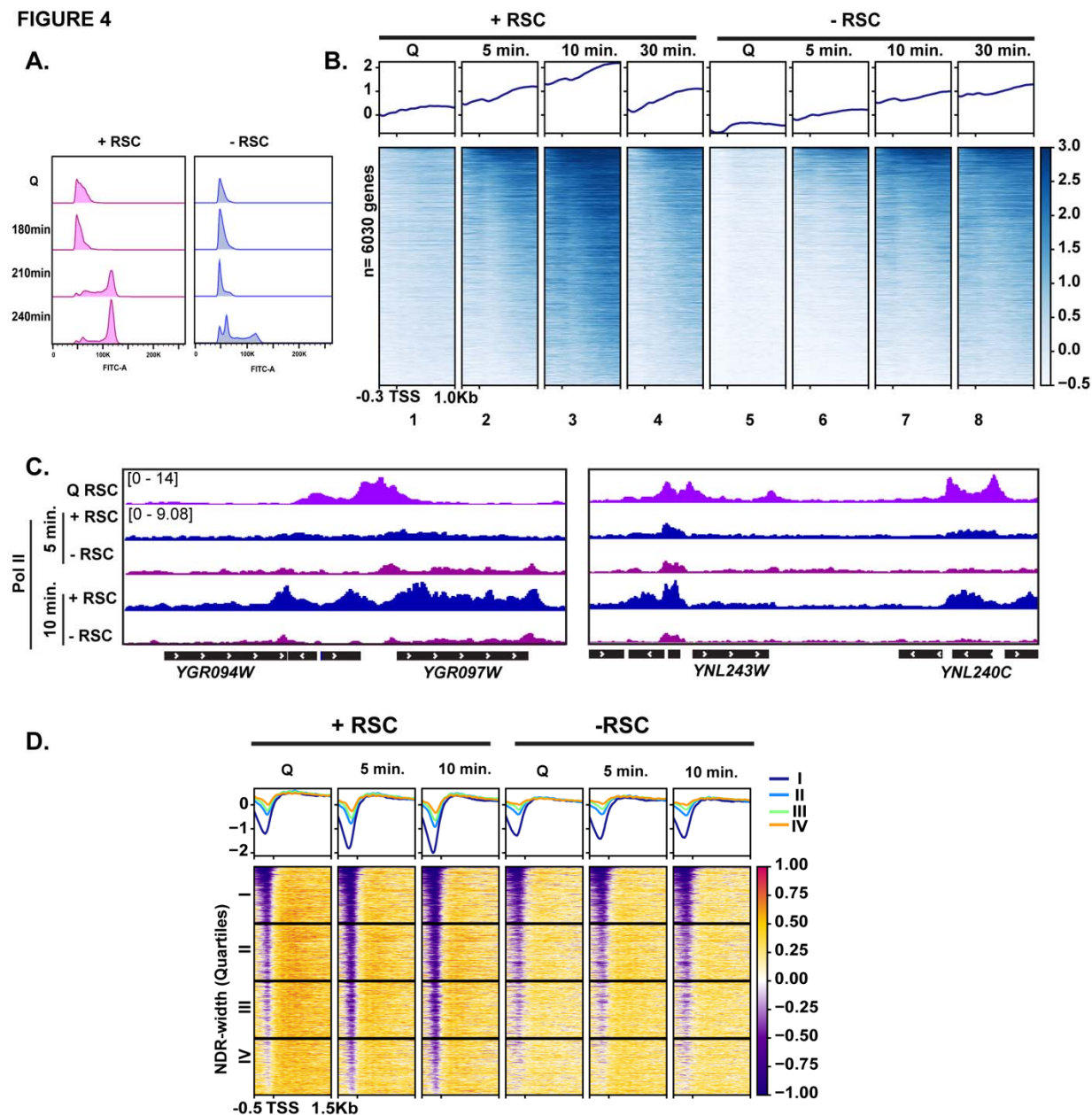


Figure 4. RSC is required for normal quiescence exit and hypertranscription upon nutrient repletion

(A) DNA content FACS analysis indicating cell cycle progression during Q exit in the presence (+) or absence (-) of RSC. **(B)** ChIP-seq analysis of Pol II across time in the presence or absence of RSC. Genes are sorted the same in all heatmaps. **(C)** Example tracks of data shown in **(B)** with RSC ChIP-seq in Q cells added. **(D)** H3 ChIP-seq sorted by NDR width (as determined by MNase-seq experiments).

FIGURE 5

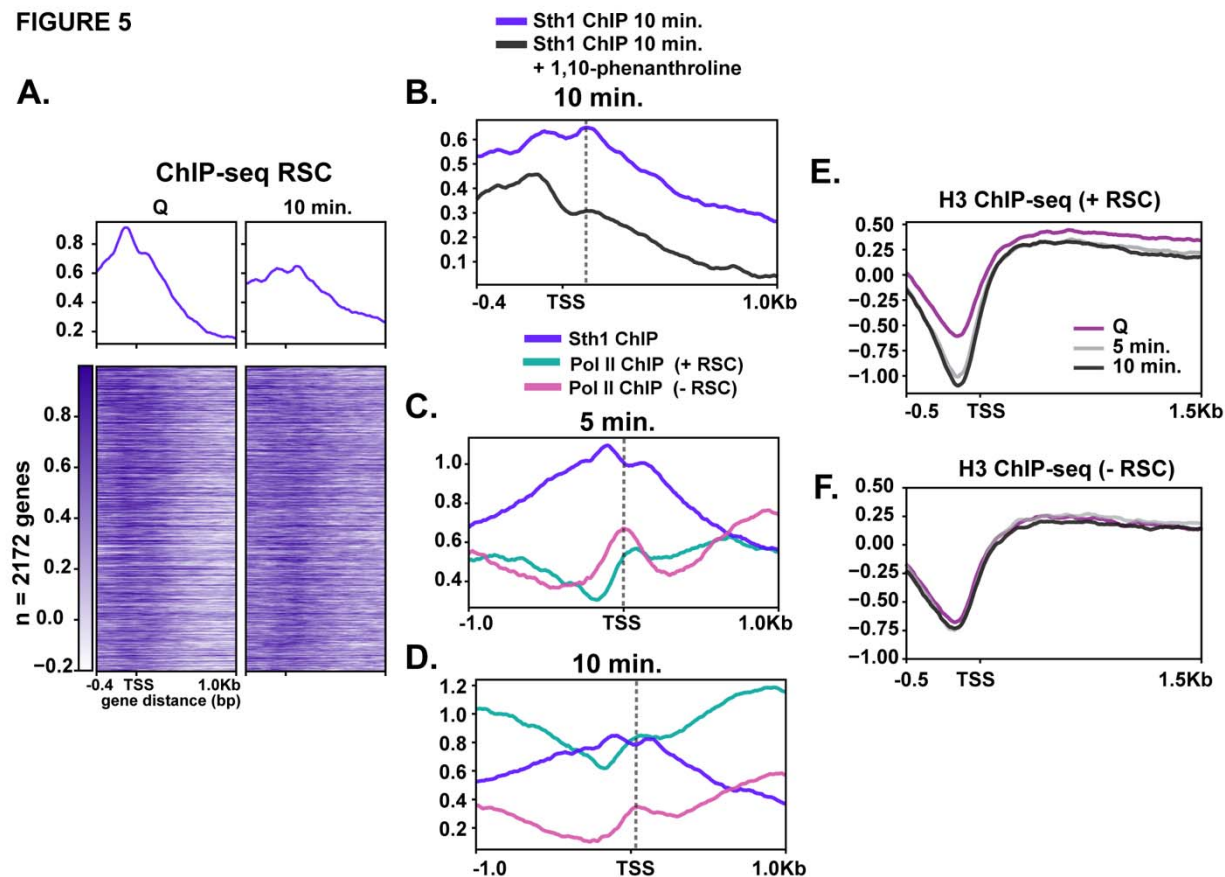


Figure 5. RSC depletion causes severe Pol II mislocalization defects during quiescence exit.

(C) ChIP-seq of RSC in Q and 10-minute time points. Genes are linked. **(B)** ChIP-seq of RSC at 10-minutes of exit in the presence and absence of the transcription inhibitor 1,10-phenanthroline. **(C, D)** ChIP-seq of RSC and Pol II during exit. **(E-F)** H3 ChIP-seq in quiescence and during exit in the presence and absence of RSC.

FIGURE 5—supplement 1

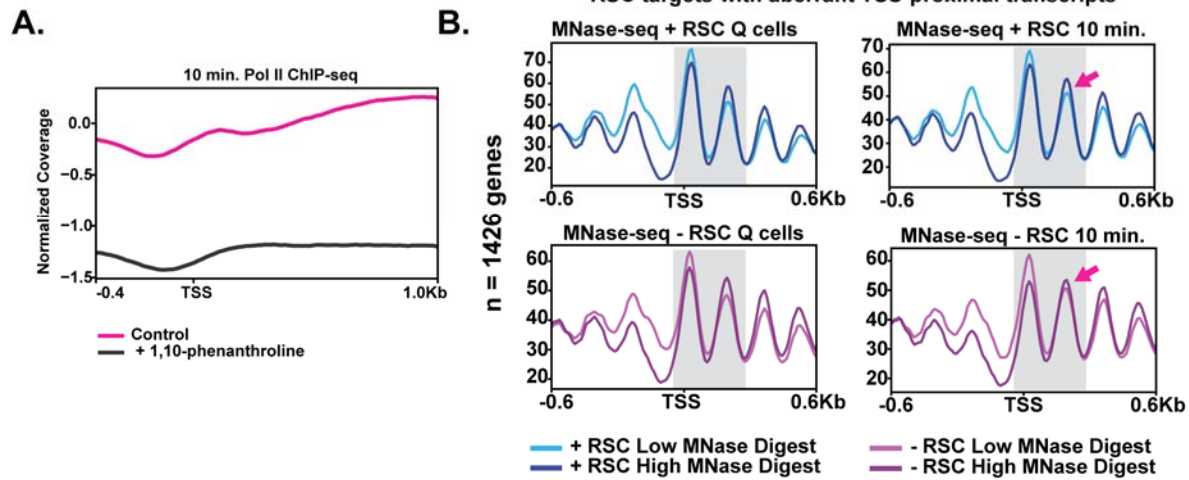


Figure 5—supplement 1

(A) ChIP-seq analysis of Pol II in the absence and presence of the transcription inhibitor 1,10-phenanthroline. **(B)** MNase-seq analysis assessing differences in MNase sensitivity in Q and ten-minutes for cells with and without RSC. The +2 nucleosome MNase-digestion differences are highlighted by the pink arrows.

FIGURE 6

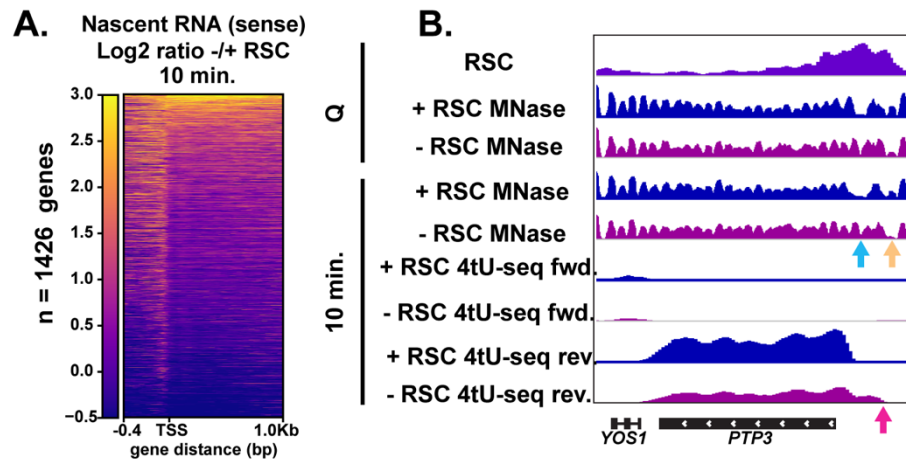


Figure 6. RSC depletion causes upstream transcription relative to canonical TSS
(A) Heatmap showing the Log₂ ratio of nascent sense transcripts in RSC-depleted versus non-depleted cells. Shown are 1426 genes that have upregulated transcripts at the 5'-ends of genes in the sense direction and have RSC ChIP signals. **(B)** Example gene of aberrant upstream transcript. Arrows direct to defects: blue arrow points to loss of NDR, yellow arrow points to gain of NDR, and pink arrow points to upstream RNA signal.

FIGURE 7

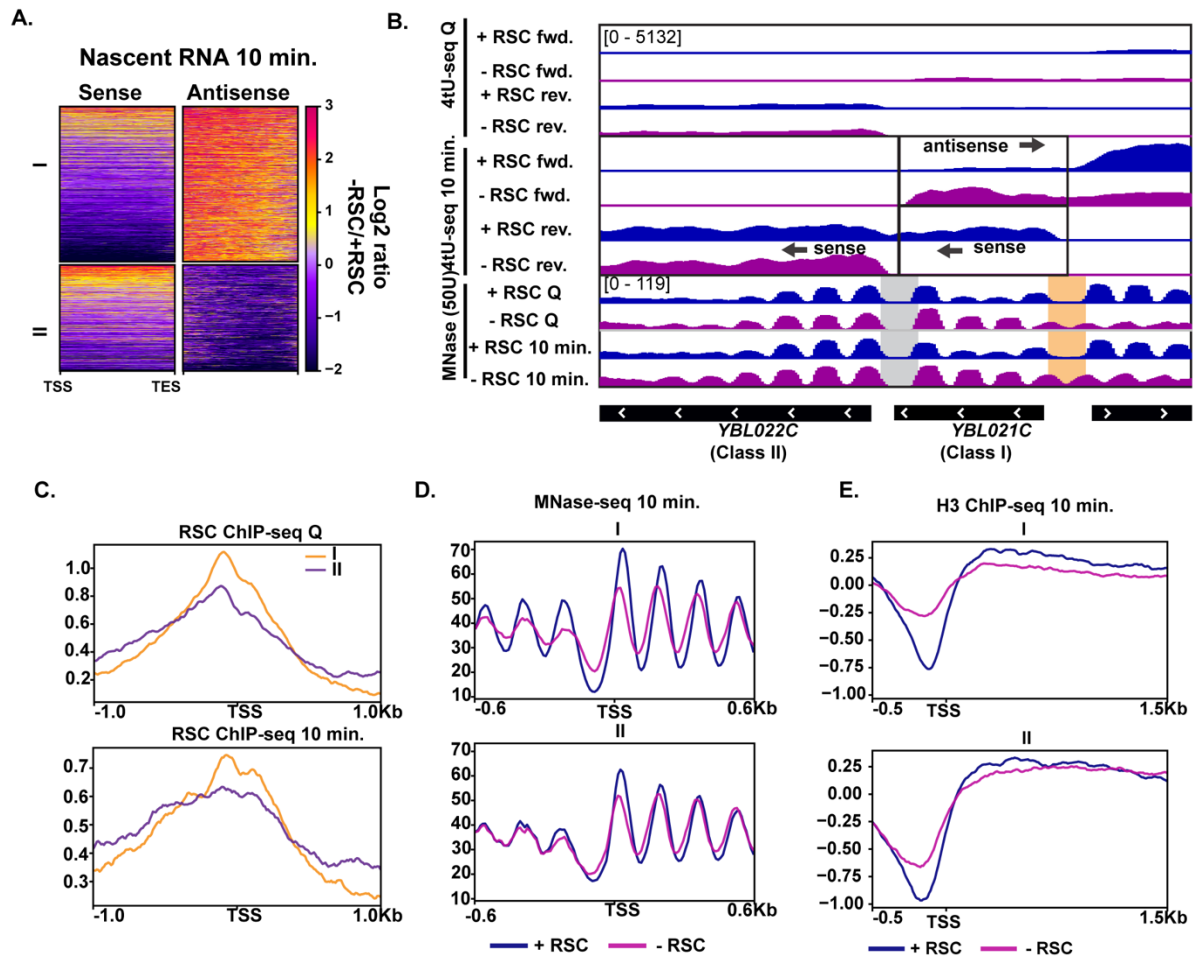


Figure 7. Aberrant antisense transcription arises when chromatin around sense transcripts is abrogated in the absence of RSC (A) Heatmaps of the Log₂ ratio of nascent RNAs that are RSC targets and give rise to antisense transcripts (cluster I, ~890 genes) when RSC is depleted and those where antisense transcripts are not made when the sense transcript NDR is unchanged (cluster II, ~600 genes). **(B)** Browser tracks of 4tU-seq and MNase-seq data. Boxes highlight defects (orange box) in NDRs and where antisense transcription arises from co-opted, intact NDRs (grey box). **(C)** ChIP-seq of RSC in quiescent cells and during exit at both cluster I and II. **(D)** MNase-seq at the 10-minute time point. **(E.)** 10-minute time point during exit of H3 ChIP-seq separated into the two clusters, I and II.

FIGURE 8

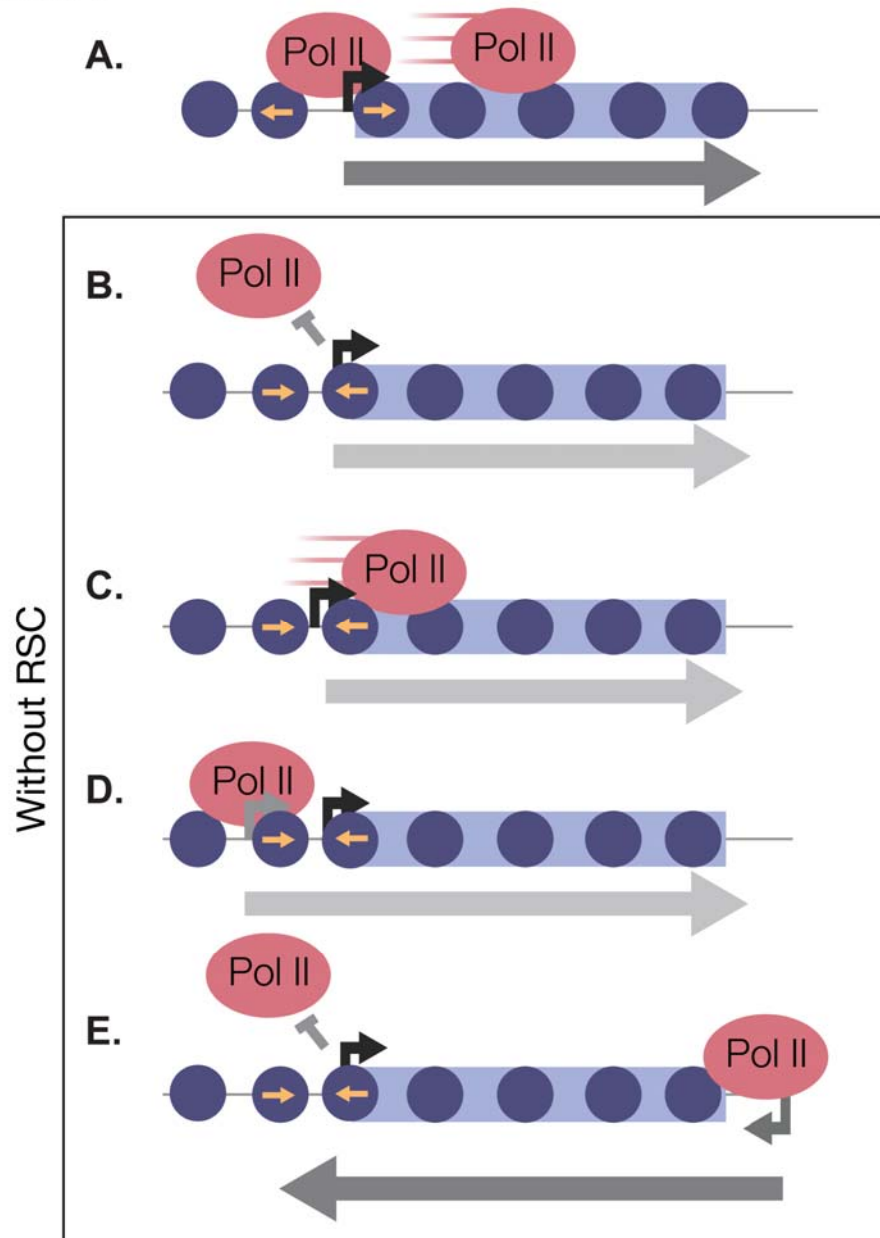


Figure 8. RSC safeguards the quiescent genome from aberrant transcription

In quiescent cells, RSC binds to NDRs upstream of Pol II transcribed genes. Upon quiescence exit, RSC shifts the +1 nucleosome to allow for Pol II occupancy and traverses into gene bodies (A). In the absence of RSC NDRs are globally narrower and transcription initiation is blocked (B). At a subset of genes, RSC is required for efficient Pol II passage past the +1 nucleosome (C) and prevent upstream TSS selection (D). NDRs that are open despite RSC depletion become cryptic promoters and are utilized by transcription machinery to generate aberrant lncRNAs and antisense transcripts (E).

References

1. Rando OJ, Winston F. Chromatin and Transcription in Yeast. *Genetics*. 2012;190: 351–387. doi:10.1534/genetics.111.132266
2. Sagot I, Laporte D. The cell biology of quiescent yeast – a diversity of individual scenarios. *J Cell Sci*. 2019;132: jcs213025. doi:10.1242/jcs.213025
3. Rittershaus ESC, Baek S-H, Sassetti CM. The Normalcy of Dormancy: Common Themes in Microbial Quiescence. *Cell Host & Microbe*. 2013;13: 643–651. doi:10.1016/j.chom.2013.05.012
4. Cheung TH, Rando TA. Molecular regulation of stem cell quiescence. *Nat Rev Mol Cell Biol*. 2013;14: 329–340. doi:10.1038/nrm3591
5. Tümpel S, Rudolph KL. Quiescence: Good and Bad of Stem Cell Aging. *Trends in Cell Biology*. 2019;29: 672–685. doi:10.1016/j.tcb.2019.05.002
6. McKnight JN, Boerma JW, Breeden LL, Tsukiyama T. Global Promoter Targeting of a Conserved Lysine Deacetylase for Transcriptional Shutoff during Quiescence Entry. *Molecular Cell*. 2015;59: 732–743. doi:10.1016/j.molcel.2015.07.014
7. Young CP, Hillyer C, Hokamp K, Fitzpatrick DJ, Konstantinov NK, Welty JS, et al. Distinct histone methylation and transcription profiles are established during the development of cellular quiescence in yeast. *BMC Genomics*. 2017;18: 107. doi:10.1186/s12864-017-3509-9
8. Swygert SG, Kim S, Wu X, Fu T, Hsieh T-H, Rando OJ, et al. Condensin-Dependent Chromatin Compaction Represses Transcription Globally during Quiescence. *Mol Cell*. 2019;73: 533-546.e4. doi:10.1016/j.molcel.2018.11.020
9. Chapman NM, Boothby MR, Chi H. Metabolic coordination of T cell quiescence and activation. *Nat Rev Immunol*. 2020;20: 55–70. doi:10.1038/s41577-019-0203-y
10. Gray JV, Petsko GA, Johnston GC, Ringe D, Singer RA, Werner-Washburne M. “Sleeping Beauty”: Quiescence in *Saccharomyces cerevisiae*. *MMBR*. 2004;68: 187–206. doi:10.1128/MMBR.68.2.187-206.2004
11. Allen C, Büttner S, Aragon AD, Thomas JA, Meirelles O, Jaetao JE, et al. Isolation of quiescent and nonquiescent cells from yeast stationary-phase cultures. *J Cell Biol*. 2006;174: 89–100. doi:10.1083/jcb.200604072
12. Luger K, Mäder AW, Richmond RK, Sargent DF, Richmond TJ. Crystal structure of the nucleosome core particle at 2.8 Å resolution. *Nature*. 1997;389: 251–260. doi:10.1038/38444

13. Lorch Y, LaPointe JW, Kornberg RD. Nucleosomes inhibit the initiation of transcription but allow chain elongation with the displacement of histones. *Cell*. 1987;49: 203–210. doi:10.1016/0092-8674(87)90561-7
14. Hainer SJ, Kaplan CD. Specialized RSC: Substrate Specificities for a Conserved Chromatin Remodeler. *BioEssays*. 2020;42: 2000002. doi:10.1002/bies.202000002
15. Cairns BR, Lorch Y, Li Y, Zhang M, Lacomis L, Erdjument-Bromage H, et al. RSC, an Essential, Abundant Chromatin-Remodeling Complex. *Cell*. 1996;87: 1249–1260. doi:10.1016/S0092-8674(00)81820-6
16. Du J, Nasir I, Benton BK, Klädde MP, Laurent BC. Sth1p, a *Saccharomyces cerevisiae* Snf2p/Swi2p homolog, is an essential ATPase in RSC and differs from Snf/Swi in its interactions with histones and chromatin-associated proteins. *Genetics*. 1998;150: 987–1005.
17. Saha A. Chromatin remodeling by RSC involves ATP-dependent DNA translocation. *Genes & Development*. 2002;16: 2120–2134. doi:10.1101/gad.995002
18. Zofall M, Persinger J, Kassabov SR, Bartholomew B. Chromatin remodeling by ISW2 and SWI/SNF requires DNA translocation inside the nucleosome. *Nat Struct Mol Biol*. 2006;13: 339–346. doi:10.1038/nsmb1071
19. Kasten M, Szerlong H, Erdjument-Bromage H, Tempst P, Werner M, Cairns BR. Tandem bromodomains in the chromatin remodeler RSC recognize acetylated histone H3 Lys14. *EMBO J*. 2004;23: 1348–1359. doi:10.1038/sj.emboj.7600143
20. Angus-Hill ML, Schlichter A, Roberts D, Erdjument-Bromage H, Tempst P, Cairns BR. A Rsc3/Rsc30 Zinc Cluster Dimer Reveals Novel Roles for the Chromatin Remodeler RSC in Gene Expression and Cell Cycle Control. *Molecular Cell*. 2001;7: 741–751. doi:10.1016/S1097-2765(01)00219-2
21. Varela I, Tarpey P, Raine K, Huang D, Ong CK, Stephens P, et al. Exome sequencing identifies frequent mutation of the SWI/SNF complex gene PBRM1 in renal carcinoma. *Nature*. 2011;469: 539–542. doi:10.1038/nature09639
22. Kadoch C, Hargreaves DC, Hodges C, Elias L, Ho L, Ranish J, et al. Proteomic and bioinformatic analysis of mammalian SWI/SNF complexes identifies extensive roles in human malignancy. *Nat Genet*. 2013;45: 592–601. doi:10.1038/ng.2628
23. Badis G, Chan ET, van Bakel H, Pena-Castillo L, Tillo D, Tsui K, et al. A Library of Yeast Transcription Factor Motifs Reveals a Widespread Function for Rsc3 in Targeting Nucleosome Exclusion at Promoters. *Molecular Cell*. 2008;32: 878–887. doi:10.1016/j.molcel.2008.11.020
24. Hartley PD, Madhani HD. Mechanisms that Specify Promoter Nucleosome Location and Identity. *Cell*. 2009;137: 445–458. doi:10.1016/j.cell.2009.02.043

25. Prajapati HK, Ocampo J, Clark DJ. Interplay among ATP-Dependent Chromatin Remodelers Determines Chromatin Organisation in Yeast. *Biology*. 2020;9: 190. doi:10.3390/biology9080190
26. Kubik S, O'Duibhir E, de Jonge WJ, Mattarocci S, Albert B, Falcone J-L, et al. Sequence-Directed Action of RSC Remodeler and General Regulatory Factors Modulates +1 Nucleosome Position to Facilitate Transcription. *Molecular Cell*. 2018;71: 89-102.e5. doi:10.1016/j.molcel.2018.05.030
27. Ng HH. Genome-wide location and regulated recruitment of the RSC nucleosome-remodeling complex. *Genes & Development*. 2002;16: 806–819. doi:10.1101/gad.978902
28. Yen K, Vinayachandran V, Batta K, Koerber RT, Pugh BF. Genome-wide Nucleosome Specificity and Directionality of Chromatin Remodelers. *Cell*. 2012;149: 1461–1473. doi:10.1016/j.cell.2012.04.036
29. Ramachandran S, Zentner GE, Henikoff S. Asymmetric nucleosomes flank promoters in the budding yeast genome. *Genome Res*. 2015;25: 381–390. doi:10.1101/gr.182618.114
30. Soutourina J, Bordas-Le Floch V, Gendrel G, Flores A, Ducrot C, Dumay-Odelot H, et al. Rsc4 Connects the Chromatin Remodeler RSC to RNA Polymerases. *MCB*. 2006;26: 4920–4933. doi:10.1128/MCB.00415-06
31. Spain MM, Ansari SA, Pathak R, Palumbo MJ, Morse RH, Govind CK. The RSC Complex Localizes to Coding Sequences to Regulate Pol II and Histone Occupancy. *Molecular Cell*. 2014;56: 653–666. doi:10.1016/j.molcel.2014.10.002
32. Biernat E, Kinney J, Dunlap K, Rizza C, Govind CK. The RSC complex remodels nucleosomes in transcribed coding sequences and promotes transcription in *Saccharomyces cerevisiae*. *Genomics*; 2020 Mar. doi:10.1101/2020.03.11.987974
33. Xi Y, Yao J, Chen R, Li W, He X. Nucleosome fragility reveals novel functional states of chromatin and poises genes for activation. *Genome Research*. 2011;21: 718–724. doi:10.1101/gr.117101.110
34. Knight B, Kubik S, Ghosh B, Bruzzone MJ, Geertz M, Martin V, et al. Two distinct promoter architectures centered on dynamic nucleosomes control ribosomal protein gene transcription. *Genes Dev*. 2014;28: 1695–1709. doi:10.1101/gad.244434.114
35. Teif VB, Beshnova DA, Vainshtein Y, Marth C, Mallm J-P, Höfer T, et al. Nucleosome repositioning links DNA (de)methylation and differential CTCF binding during stem cell development. *Genome Res*. 2014;24: 1285–1295. doi:10.1101/gr.164418.113
36. Kubik S, Bruzzone MJ, Jacquet P, Falcone J-L, Rougemont J, Shore D. Nucleosome Stability Distinguishes Two Different Promoter Types at All Protein-

- Coding Genes in Yeast. *Molecular Cell*. 2015;60: 422–434.
doi:10.1016/j.molcel.2015.10.002
37. Floer M, Wang X, Prabhu V, Berrozpe G, Narayan S, Spagna D, et al. A RSC/Nucleosome Complex Determines Chromatin Architecture and Facilitates Activator Binding. *Cell*. 2010;141: 407–418. doi:10.1016/j.cell.2010.03.048
 38. Brahma S, Henikoff S. RSC-Associated Subnucleosomes Define MNase-Sensitive Promoters in Yeast. *Molecular Cell*. 2019;73: 238-249.e3.
doi:10.1016/j.molcel.2018.10.046
 39. Schlichter A, Kasten MM, Parnell TJ, Cairns BR. Specialization of the chromatin remodeler RSC to mobilize partially-unwrapped nucleosomes. *eLife*. 2020;9: e58130. doi:10.7554/eLife.58130
 40. Percharde M, Bulut-Karslioglu A, Ramalho-Santos M. Hypertranscription in Development, Stem Cells, and Regeneration. *Developmental Cell*. 2017;40: 9–21.
doi:10.1016/j.devcel.2016.11.010
 41. Miller C, Schwalb B, Maier K, Schulz D, Dümcke S, Zacher B, et al. Dynamic transcriptome analysis measures rates of mRNA synthesis and decay in yeast. *Mol Syst Biol*. 2011;7: 458. doi:10.1038/msb.2010.112
 42. Duffy EE, Rutenberg-Schoenberg M, Stark CD, Kitchen RR, Gerstein MB, Simon MD. Tracking Distinct RNA Populations Using Efficient and Reversible Covalent Chemistry. *Molecular Cell*. 2015;59: 858–866. doi:10.1016/j.molcel.2015.07.023
 43. Radonjic M, Andrau J-C, Lijnzaad P, Kemmeren P, Kockelkorn TTJP, van Leenen D, et al. Genome-Wide Analyses Reveal RNA Polymerase II Located Upstream of Genes Poised for Rapid Response upon *S. cerevisiae* Stationary Phase Exit. *Molecular Cell*. 2005;18: 171–183. doi:10.1016/j.molcel.2005.03.010
 44. Mews P, Zee BM, Liu S, Donahue G, Garcia BA, Berger SL. Histone Methylation Has Dynamics Distinct from Those of Histone Acetylation in Cell Cycle Reentry from Quiescence. *Molecular and Cellular Biology*. 2014;34: 3968–3980.
doi:10.1128/MCB.00763-14
 45. Martin BJE, Brind'Amour J, Kuzmin A, Jensen KN, Liu ZC, Lorincz M, et al. Transcription shapes genome-wide histone acetylation patterns. *Nat Commun*. 2021;12: 210. doi:10.1038/s41467-020-20543-z
 46. Noe Gonzalez M, Blears D, Svejstrup JQ. Causes and consequences of RNA polymerase II stalling during transcript elongation. *Nat Rev Mol Cell Biol*. 2021;22: 3–21. doi:10.1038/s41580-020-00308-8
 47. Churchman LS, Weissman JS. Nascent transcript sequencing visualizes transcription at nucleotide resolution. *Nature*. 2011;469: 368–373.
doi:10.1038/nature09652

48. Hubert JC, Guyonvarch A, Kammerer B, Exinger F, Liljelund P, Lacroute F. Complete sequence of a eukaryotic regulatory gene. *The EMBO Journal*. 1983;2: 2071–2073. doi:10.1002/j.1460-2075.1983.tb01702.x
49. Vinayachandran V, Reja R, Rossi MJ, Park B, Rieber L, Mittal C, et al. Widespread and precise reprogramming of yeast protein–genome interactions in response to heat shock. *Genome Res*. 2018;28: 357–366. doi:10.1101/gr.226761.117
50. Parnell TJ, Huff JT, Cairns BR. RSC regulates nucleosome positioning at Pol II genes and density at Pol III genes. *EMBO J*. 2008;27: 100–110. doi:10.1038/sj.emboj.7601946
51. Mahapatra S, Dewari PS, Bhardwaj A, Bhargava P. Yeast H2A.Z, FACT complex and RSC regulate transcription of tRNA gene through differential dynamics of flanking nucleosomes. *Nucleic Acids Research*. 2011;39: 4023–4034. doi:10.1093/nar/gkq1286
52. Kumar Y, Bhargava P. A unique nucleosome arrangement, maintained actively by chromatin remodelers facilitates transcription of yeast tRNA genes. *BMC Genomics*. 2013;14: 402. doi:10.1186/1471-2164-14-402
53. Nishimura K, Kanemaki MT. Rapid Depletion of Budding Yeast Proteins via the Fusion of an Auxin-Inducible Degron (AID). *Current Protocols in Cell Biology*. 2014;64. doi:10.1002/0471143030.cb2009s64
54. Tsuchiya E, Uno M, Kiguchi A, Masuoka K, Kanemori Y, Okabe S, et al. The *Saccharomyces cerevisiae* NPS1 gene, a novel CDC gene which encodes a 160 kDa nuclear protein involved in G2 phase control. *EMBO J*. 1992;11: 4017–4026.
55. Kubik S, Bruzzone MJ, Challal D, Dreos R, Mattarocci S, Bucher P, et al. Opposing chromatin remodelers control transcription initiation frequency and start site selection. *Nat Struct Mol Biol*. 2019;26: 744–754. doi:10.1038/s41594-019-0273-3
56. Klein-Brill A, Joseph-Strauss D, Appleboim A, Friedman N. Dynamics of Chromatin and Transcription during Transient Depletion of the RSC Chromatin Remodeling Complex. *Cell Reports*. 2019;26: 279-292.e5. doi:10.1016/j.celrep.2018.12.020
57. Ocampo J, Chereji RV, Eriksson PR, Clark DJ. Contrasting roles of the RSC and ISW1/CHD1 chromatin remodelers in RNA polymerase II elongation and termination. *Genome Res*. 2019;29: 407–417. doi:10.1101/gr.242032.118
58. Spain MM, Bracerós KCA, Tsukiyama T, Fred Hutchinson Cancer Research Center, Division of Basic Sciences. SWI/SNF coordinates transcriptional activation through Rpd3-mediated histone hypoacetylation during quiescence entry. *Molecular Biology*; 2018 Sep. doi:10.1101/426288

59. Poramba-Liyanage DW, Korthout T, Cucinotta CE, van Kruijsbergen I, van Welsem T, El Atmioui D, et al. Inhibition of transcription leads to rewiring of locus-specific chromatin proteomes. *Genome Res.* 2020;30: 635–646. doi:10.1101/gr.256255.119
60. Kireeva ML, Hancock B, Cremona GH, Walter W, Studitsky VM, Kashlev M. Nature of the Nucleosomal Barrier to RNA Polymerase II. *Molecular Cell.* 2005;18: 97–108. doi:10.1016/j.molcel.2005.02.027
61. Bondarenko VA, Steele LM, Újvári A, Gaykalova DA, Kulaeva OI, Polikanov YS, et al. Nucleosomes Can Form a Polar Barrier to Transcript Elongation by RNA Polymerase II. *Molecular Cell.* 2006;24: 469–479. doi:10.1016/j.molcel.2006.09.009
62. Lorch Y, Maier-Davis B, Kornberg RD. Histone Acetylation Inhibits RSC and Stabilizes the +1 Nucleosome. *Molecular Cell.* 2018;72: 594-600.e2. doi:10.1016/j.molcel.2018.09.030
63. Ye Y, Wu H, Chen K, Clapier CR, Verma N, Zhang W, et al. Structure of the RSC complex bound to the nucleosome. *Science.* 2019;366: 838–843. doi:10.1126/science.aay0033
64. Patel AB, Moore CM, Greber BJ, Luo J, Zukin SA, Ranish J, et al. Architecture of the chromatin remodeler RSC and insights into its nucleosome engagement. *eLife.* 2019;8: e54449. doi:10.7554/eLife.54449
65. Wagner FR, Dienemann C, Wang H, Stützer A, Tegunov D, Urlaub H, et al. Structure of SWI/SNF chromatin remodeller RSC bound to a nucleosome. *Nature.* 2020;579: 448–451. doi:10.1038/s41586-020-2088-0
66. Baker RW, Reimer JM, Carman PJ, Turegun B, Arakawa T, Dominguez R, et al. Structural insights into assembly and function of the RSC chromatin remodeling complex. *Nat Struct Mol Biol.* 2021;28: 71–80. doi:10.1038/s41594-020-00528-8
67. Shogren-Knaak M. Histone H4-K16 Acetylation Controls Chromatin Structure and Protein Interactions. *Science.* 2006;311: 844–847. doi:10.1126/science.1124000
68. Robinson PJJ, An W, Routh A, Martino F, Chapman L, Roeder RG, et al. 30 nm Chromatin Fibre Decompaction Requires both H4-K16 Acetylation and Linker Histone Eviction. *Journal of Molecular Biology.* 2008;381: 816–825. doi:10.1016/j.jmb.2008.04.050
69. Allahverdi A, Yang R, Korolev N, Fan Y, Davey CA, Liu C-F, et al. The effects of histone H4 tail acetylations on cation-induced chromatin folding and self-association. *Nucleic Acids Research.* 2011;39: 1680–1691. doi:10.1093/nar/gkq900

70. Swygert SG, Lin D, Portillo-Ledesma S, Lin P-Y, Hunt DR, Kao C-F, et al. Chromatin Fiber Folding Represses Transcription and Loop Extrusion in Quiescent Cells. *Molecular Biology*; 2020 Nov. doi:10.1101/2020.11.24.396713
71. Rawal Y, Chereji RV, Qiu H, Ananthakrishnan S, Govind CK, Clark DJ, et al. SWI/SNF and RSC cooperate to reposition and evict promoter nucleosomes at highly expressed genes in yeast. *Genes Dev.* 2018;32: 695–710. doi:10.1101/gad.312850.118
72. Han P, Chang C-P. Long non-coding RNA and chromatin remodeling. *RNA Biology.* 2015;12: 1094–1098. doi:10.1080/15476286.2015.1063770
73. Alcid EA, Tsukiyama T. ATP-dependent chromatin remodeling shapes the long noncoding RNA landscape. *Genes Dev.* 2014;28: 2348–2360. doi:10.1101/gad.250902.114
74. Marquardt S, Escalante-Chong R, Pho N, Wang J, Churchman LS, Springer M, et al. A Chromatin-Based Mechanism for Limiting Divergent Noncoding Transcription. *Cell.* 2014;157: 1712–1723. doi:10.1016/j.cell.2014.04.036
75. Gill JK, Maffioletti A, García-Molinero V, Stutz F, Soudet J. Fine Chromatin-Driven Mechanism of Transcription Interference by Antisense Noncoding Transcription. *Cell Reports.* 2020;31: 107612. doi:10.1016/j.celrep.2020.107612
76. Hainer SJ, Gu W, Carone BR, Landry BD, Rando OJ, Mello CC, et al. Suppression of pervasive noncoding transcription in embryonic stem cells by esBAF. *Genes Dev.* 2015;29: 362–378. doi:10.1101/gad.253534.114
77. Thomas BJ, Rothstein R. The genetic control of direct-repeat recombination in *Saccharomyces*: the effect of *rad52* and *rad1* on mitotic recombination at *GAL10*, a transcriptionally regulated gene. *Genetics.* 1989;123: 725–738.
78. Ausubel FM, B.R. Kingston RE, Moore DD, Seidman JG, Smith JA, Struhl K. *Current Protocols in Molecular Biology.* 1988; NYWiley-Interscience.
79. Cox JS, Chapman RE, Walter P. The unfolded protein response coordinates the production of endoplasmic reticulum protein and endoplasmic reticulum membrane. *MBoC.* 1997;8: 1805–1814. doi:10.1091/mbc.8.9.1805
80. Rodriguez J, McKnight JN, Tsukiyama T. Genome-Wide Analysis of Nucleosome Positions, Occupancy, and Accessibility in Yeast: Nucleosome Mapping, High-Resolution Histone ChIP, and NCAM. *Current Protocols in Molecular Biology.* 2014;108. doi:10.1002/0471142727.mb2128s108
81. Langmead B, Salzberg SL. Fast gapped-read alignment with Bowtie 2. *Nat Methods.* 2012;9: 357–359. doi:10.1038/nmeth.1923

82. Li H, Handsaker B, Wysoker A, Fennell T, Ruan J, Homer N, et al. The Sequence Alignment/Map format and SAMtools. *Bioinformatics*. 2009;25: 2078–2079. doi:10.1093/bioinformatics/btp352
83. Ramírez F, Dünder F, Diehl S, Grüning BA, Manke T. deepTools: a flexible platform for exploring deep-sequencing data. *Nucleic Acids Research*. 2014;42: W187–W191. doi:10.1093/nar/gku365
84. Xu Y, Bernecky C, Lee C-T, Maier KC, Schwalb B, Tegunov D, et al. Architecture of the RNA polymerase II-Paf1C-TFIIS transcription elongation complex. *Nat Commun*. 2017;8: 15741. doi:10.1038/ncomms15741
85. Bonnet J, Wang C-Y, Baptista T, Vincent SD, Hsiao W-C, Stierle M, et al. The SAGA coactivator complex acts on the whole transcribed genome and is required for RNA polymerase II transcription. *Genes Dev*. 2014;28: 1999–2012. doi:10.1101/gad.250225.114
86. Love MI, Huber W, Anders S. Moderated estimation of fold change and dispersion for RNA-seq data with DESeq2. *Genome Biol*. 2014;15: 550. doi:10.1186/s13059-014-0550-8